

Thermodynamic Properties of Impure Heisenberg Antiferromagnets

L. R. Walker and B. C. Chambers
Bell Telephone Laboratories, Murray Hill, New Jersey 07974

and

D. Hone*
Department of Physics, University of California, Santa Barbara, California 93106

and

Herbert Callen†
Department of Physics, University of Pennsylvania, Philadelphia, Pennsylvania 19104
 (Received 16 September 1971)

The local thermodynamic properties of Heisenberg antiferromagnets with dilute substitutional impurities are studied by Green's-function techniques within the random-phase approximation (RPA). A body-centered two-sublattice model, with a single exchange constant and a single-ion staggered-anisotropy field, is used. A representative set of impurity exchange and spin magnitudes is chosen for quantitative study. The spectral distribution of spin excitations, including localized mode contributions, the zero-point spin deviation, and the temperature dependence of the magnetization are examined for the impurity and its first four shells of neighbors. Within the limitations of the single-exchange model (and of the RPA) a comparison is made with resonance and optical experiments on Zn, Fe, and Ni impurities in MnF_2 . Good agreement was found in the first two cases, but no successful fit to the Ni data was possible, perhaps reflecting the importance of the substantial additional exchange with near neighbors in this case.

I. INTRODUCTION

A number of papers have discussed the effect of replacing a single spin in a Heisenberg antiferromagnetic by one of different magnetic properties.¹ The problem has much in common with that of impurities in ferromagnets,^{2,3} or with that of the effect of foreign atoms on phonon spectra. The effects upon the excitation spectrum of the systems are, in all cases, much the same. If some suitable spectral density is defined to measure the excitation strength at any site, this will have some characteristic form within the continuum of pure-host excitations. On introduction of the impurity this spectral density is radically modified at the impurity and to a lesser extent on near-neighbor sites. Peaks may occur within the continuum and these are usually referred to as resonances. They may be of any degree of sharpness; if they are very narrow they become experimentally indistinguishable from localized levels. The latter occur in some circumstances outside the host continuum and, in simple theories which neglect damping, are perfectly sharp. Since anisotropic antiferromagnets have an energy gap, such local modes may occur below the continuum as well as above. All excitations of the impure system must reflect the point-group symmetry of the impurity and may be classified accordingly. The resonance phenomenon and the sharp levels will occur within the excita-

tions of a particular symmetry, and it is appropriate to refer to them as resonant or localized *modes* of that symmetry.

The alteration of the excitation spectrum of the spin system by the impurity changes the thermodynamic properties of the whole system. Far from the impurity one expects to see little change in the thermal behavior of a host spin, but in its immediate neighborhood some modification must take place. The impurity itself will clearly behave unlike a host spin. The problem treated here is that of evaluating the temperature dependence of the impurity magnetization and that of a few shells of neighbors. We know that for the pure host a reliable calculation of the sublattice magnetization can be made at low temperatures and, by means of various renormalization schemes, less reliable estimates can be given right up to the Curie temperature. In the impurity problem the first part of this statement remains true, but the extension to higher temperatures becomes more uncertain. One reason for this is that the presence of the impurity has changed the local excitation spectrum and this, in turn, modifies the various spin averages at different sites. The medium has now, in effect, been modified and this alters the excitation spectrum. The whole problem should therefore be solved in a self-consistent way within any approximation scheme such as the random-phase approximation (RPA). This is prohibitively difficult. It is there-

fore necessary to assume that the effect of the impurity on the spin averages in its neighborhood is both small and of limited range. If this is the case, it is possible to derive an answer and this may then be examined to see whether it is consistent with these assumptions. It appears that for a substantial temperature range, this is, in fact, the case. Note, however, that this is verified only for the particular approximation used, which in the present case was the RPA. Clearly, such a verification lends no support to the RPA decoupling itself.

A more important limitation is that approximation schemes, such as the RPA, may have a narrower range of applicability for the impurity problem than for the case of a pure host. Some evidence that this is, in fact, true will be pointed out later.

II. MODEL

In the limit of extreme dilution the impurities act independently, and the theoretical problem is conveniently simplified to consideration of a single impurity in an otherwise perfect crystal. The validity of such an approximation relies on the effective range of interaction between impurities being smaller than their average separation at experimentally useful concentrations. In insulators, the exchange forces themselves have a short range, so one must worry primarily about the modification of the host medium about one impurity which may be felt by a second. As pointed out in the Introduction, these effects do appear to drop off rather rapidly with distance.

We have chosen to examine the two- (magnetic) sublattice bcc crystal, with the "up" spins, say, occupying the body-center sites and the "down" spins occupying the cube corners. The results, however, are applicable to any body-centered lattice, since only the topology of the structure is critical in the analysis. The effective Hamiltonian of the system is taken to be given in terms of spin operators associated with each lattice site; explicitly, orbital effects are ignored. The interaction between spins S_i and S_j on sites i and j is described by isotropic Heisenberg exchange ($J_{ij}\vec{S}_i \cdot \vec{S}_j$), and the number of parameters in the model is reduced by taking only a single nonvanishing-exchange integral J_{ij} —that between a spin and its nearest neighbors on the opposite sublattice. We represent the effect of crystalline anisotropy in terms of an anisotropy field $-g_i\mu_B H_i^A S_i^z$ (g_i is the g factor of the i th spin), which again simplifies the analysis. The field H_i^A must, of course, be staggered or reversed in sign from one sublattice to the other for the host spins; for the impurity it may have either sign. It must fall off in magnitude as the temperature increases toward T_N ; we have taken it usually to be proportional to the magnetization $\langle S_i^z \rangle$ at the site on which it acts. We point out that our procedures

may be readily modified to accommodate any other, more realistic, temperature dependence of H_i^A . Only systems in zero applied magnetic fields will be considered in this paper in order to avoid considerable algebraic complication.

The Hamiltonian, then, is of the general form

$$\mathcal{H} = \sum_{i,j} J_{ij} \vec{S}_i \cdot \vec{S}_j - \sum_i K_i \langle S_i^z \rangle S_i^z. \quad (2.1)$$

The host is characterized by the magnitude of each spin S , by the single nonvanishing-exchange integral J between nearest neighbors on different sublattices, and by the anisotropy constant K . The results will depend parametrically on S , J , and K and on the corresponding quantities S' , J' , and K' associated with the impurity which has substitutionally replaced one of the host spins. We assume that only the impurity nearest-neighbor exchange integral differs from the host value. It should be noted that there is evidence in some cases that this may not be valid.⁴

III. GREEN'S FUNCTIONS

The most convenient tool for studying the thermodynamic behavior of the spins is the two-time thermodynamic Green's function. Use has been made of the function $G_{ij}(t)$ defined by

$$G_{ij}(t) = -i\theta(t) \langle [S_i^z(t), S_j^z(0)] \rangle, \quad (3.1)$$

where $\theta(t)$ is the unit step function, the operators are given in the Heisenberg representation, and the angular brackets denote the thermodynamic ensemble average of the expectation value of the operator within. The square brackets indicate a commutator. These functions are discussed in detail in a variety of references; here we wish to emphasize only their properties that bear directly on the present calculation.

$G_{ij}(t)$ measures the response at time t of the spin at site i to a field which flips the spin at j at time $t=0$. Its behavior is more readily interpreted from its spectral representation (time Fourier transform):

$$G_{ij}(E) = \frac{1}{Z} \int \frac{dE'}{2\pi} \times \sum_{\alpha,\gamma} \frac{e^{-\beta E_\alpha} (1 - e^{-\beta E'}) \langle \alpha | S_i^z | \gamma \rangle \langle \gamma | S_j^z | \alpha \rangle}{E - E' + i0^+} \times \delta(E' - E_\gamma + E_\alpha), \quad (3.2)$$

where α and γ are summed over the *exact* eigenstates of the Hamiltonian of energy E_α ; $\beta = 1/kT$, $Z = \sum_\alpha e^{-\beta E_\alpha}$. Thus the poles of $G_{ij}(E)$ occur at the exact excitation energies of the system, with residues characterized by matrix elements which measure the probability amplitudes that the spins at i and j are flipped by these excitations. From the

standard dispersion relation form of Eq. (3.2) it is clear that all information is contained in the discontinuity of $G_{ij}(E)$ across the real E axis

$$\lim_{\epsilon \rightarrow 0} [G_{ij}(E+i\epsilon) - G_{ij}(E-i\epsilon)] = -i(1 - e^{-\beta E})A_{ij}(E), \quad (3.3)$$

where the spectral-weight function $A_{ij}(E)$ is defined by

$$A_{ij}(E) = \frac{1}{Z} \sum_{\alpha, \gamma} e^{-\beta E \alpha} \langle \alpha | S_i^+ | \gamma \rangle \langle \gamma | S_j^- | \alpha \rangle \delta(E - E_{\gamma\alpha}). \quad (3.4)$$

Then the full Green's functions are recovered from

$$G_{ij}(E) = \int \frac{dE'}{2\pi} \frac{(1 - e^{-\beta E'})A_{ij}(E')}{E - E' + i0^+}. \quad (3.5)$$

The diagonal elements A_{ii} are of particular interest; they measure the probability of flipping the spin at i with energy E . In the limit of a large system the eigenvalues coalesce to describe a quasi-continuous spin-wave band. If this limit is taken before the imaginary part of the energy is taken to zero, then the $A_{ii}(E)$ are smooth functions (rather than sums of δ functions) representing the integrated contribution over many excitations, where each is of energy very nearly E . These functions thus have folded into them an energy density of excitations, as well as the factor of the spin-flip probability at the site i due to these excitations. The A_{ij} satisfy a useful set of sum rules, which are an immediate consequence of the commutation relations of the spin operators

$$2 \langle S_i^z \rangle \delta_{ij} = iG_{ij}(t=0^+) = \int_{-\infty}^{\infty} dE (1 - e^{-\beta E}) A_{ij}(E). \quad (3.6)$$

The sum rules do not provide a means of finding $\langle S_i^z \rangle$, since within the approximation we use for decoupling the equations of motion for G_{ij} , those equations are linear in the G 's and the inhomogeneous driving term is proportional to $\langle S_j^z \rangle$, so that the $G_{ij}(\omega)$ are inevitably proportional to $\langle S_i^z \rangle$. However, the equality which survives when $\langle S_i^z \rangle$ is cancelled out of Eq. (3.6) is extremely useful as a check for the numerical analysis, as will be emphasized below. Equation (3.6) was derived for the exact Green's functions, but we show in Sec. IV that it is valid for the type of approximation we have used.

To determine $\langle S_i^z \rangle$ from $A_{ii}(E)$ we have used the algorithms proved first by Callen⁵ and later generalized by Callen and Shtrikman.⁶ They showed that in renormalized spin-wave approximations (of which the RPA is one) the magnetization $\langle S_i^z \rangle$ is given by

$$\langle S_i^z \rangle = S_i B_{S_i}(\beta \Omega_i), \quad (3.7)$$

where $B_{S_i}(x)$ is the Brillouin function for spin magnitude S_i . It is defined by

$$B_{S_i} = \frac{2S_i + 1}{2S_i} \coth(S_i + \frac{1}{2})x - \frac{1}{2S_i} \coth \frac{1}{2}x \quad (3.8)$$

and Ω_i is the energy of a "quasiboson" determined from

$$\frac{1}{e^{\beta \Omega_i} - 1} = \int_{-\infty}^{+\infty} \frac{dE}{e^{\beta E} - 1} \frac{\text{Im } G_{ii}(E)}{\langle S_i^z \rangle}. \quad (3.9)$$

Note that, under the special conditions where $G_{ii}(E)$ is sharply peaked at some E which is proportional to $\langle S_i^z \rangle$, the above procedure leads to molecular field theory.

It is of some interest to take special note at this stage of the zero-point deviation of the magnetization in this formalism. In the limit of zero temperature Eq. (3.7) becomes

$$\begin{aligned} \lim_{\beta \rightarrow \infty} (e^{\beta \Omega_i} - 1)^{-1} &= \sum_{\alpha} \int_{-\infty}^{\infty} dE |\langle \alpha | S_i^+ | 0 \rangle|^2 \delta(E + E_{\alpha}) \\ &= \frac{1}{2 \langle S_i^z \rangle} \langle 0 | S_i^- S_i^+ | 0 \rangle, \end{aligned} \quad (3.10)$$

where $|0\rangle$ is the ground state and the energies are referred to that of the ground state. Whereas for the ferromagnet $S_i^+ |0\rangle = 0$, so that $\beta \Omega_i \rightarrow \infty$ and $\langle S_i^z \rangle = S_i$ (the ground state is fully aligned), this is not so for the antiferromagnet. An "up" spin i can be flipped up further from the ground state with non-vanishing probability. We point out that this information is all contained in $A_{ii}(E)$ for *negative* E . This part of $A_{ii}(E)$ is not only identically zero for the ferromagnet at $T=0^\circ\text{K}$; it also vanishes at *finite* temperature in renormalized spin-wave approximations. The turning down of the spin at i is then some linear combination of the creation of the various renormalized spin waves. In the corresponding approximations in the antiferromagnet, however, the flipping down of an "up" spin decomposes in part into spin waves which primarily have amplitude on the "down" sublattice. Since the spins are being flipped *down*, this part of the decomposition must correspond (with the exception of restoration of the small zero-point deviation) to *destruction* of a spin wave and thus to a negative energy contribution to the spectral-weight function.

In order to avoid any confusion about signs we recapitulate some salient facts. The spectral weight function A_{ii} is positive by definition. $\text{Im } G \propto -\frac{1}{2}(1 - e^{-\beta E})A_{ii}$ is negative for $E > 0$ and positive for $E < 0$. The sum rule $-\int \text{Im } G_{ii} dE = \langle S_i^z \rangle$ is made up of a positive quantity from $0 < E < \infty$ and a negative quantity from $-\infty < E < 0$. The spin deviation is given for small deviations as proportional to $-\int_{-\infty}^{+\infty} \text{Im } G/e^{\beta E} - 1 dE$, and its positive and negative energy contributions are both positive. The last statement holds for "up" sites; there is an analogous proposition for down sites.

IV. GENERAL FEATURES

A. Equation of Motion

The equation of motion of the Green's functions $G_{lm}(t)$ is

$$i \frac{\partial}{\partial t} G_{lm}(t) = 2 \langle S_m^z \rangle \delta_{lm} \delta(t) - i\theta(t) \langle [S_l^+, H]_t, S_m^-(0) \rangle, \quad (4.1)$$

where the subscript t indicates that the value is taken at time t . With the general form of the Hamiltonian (2.1) this yields

$$i \frac{\partial}{\partial t} G_{lm}(t) = 2 \langle S_m^z \rangle \delta_{lm} \delta(t) + K_l \langle S_l^z \rangle G_{lm}(t) - 2i\theta(t) \sum_{k(l)} J_{lk} \langle [S_l^+ S_k^+]_t, S_m^-(0) - (S_l^+ S_k^+)_t, S_m^-(0) \rangle.$$

The notation $k(l)$ will be used to denote sites k which are nearest neighbors on the opposite sublattice of a specific site l . The simplest RPA-decoupling scheme, in which a term such as $\langle [S_l^+ S_k^+]_t, S_m^-(0) \rangle$ is approximated by $\langle S_l^z \rangle \langle [S_k^+, S_m^-(0)] \rangle$ has been used. This seemed reasonable in an exploratory analysis of this type, but there are some very cogent objections to it which will be discussed in Sec. VII. With this approximation, Eq. (4.1) becomes

$$i \frac{\partial}{\partial t} G_{lm}(t) = 2 \langle S_m^z \rangle \delta_{lm}(t) + K_l \langle S_l^z \rangle G_{lm}(t) + 2 \sum_{k(l)} J_{lk} [\langle S_l^z \rangle G_{km}(t) - \langle S_k^z \rangle G_{lm}(t)]. \quad (4.2)$$

If the time Fourier transform $G_{lm}(E)$ of $G_{lm}(t)$ is introduced, where

$$G_{lm}(E) = \frac{1}{2\pi} \int_{-\infty}^{+\infty} e^{iEt} G_{lm}(t) dt, \quad (4.3)$$

with \hbar set equal to unity, one obtains

$$EG_{lm}(E) = 2\delta_{lm} \left(\frac{\langle S_m^z \rangle}{\pi} \right) + K_l \langle S_l^z \rangle G_{lm}(E) + 2 \sum_{k(l)} J_{lk} [\langle S_l^z \rangle G_{km}(E) - \langle S_k^z \rangle G_{lm}(E)]. \quad (4.4)$$

Let an arbitrary site of the up lattice be designated by the subscript g and one on the down sublattice by the subscript f . In the pure host or at great distances from the impurity one will have

$$\langle S_g^z \rangle = -\langle S_f^z \rangle = S_\infty, \quad (4.5)$$

where S_∞ is the sublattice magnetization of the normal host crystal. It is now convenient to introduce the following normalized variables appropriate to the body-centered structure:

$$\epsilon = (16 JS_\infty)^{-1} E, \quad \alpha = (16 J)^{-1} K, \\ \alpha_l = (16 J)^{-1} K_l, \quad j_{lm} = J^{-1} J_{lm},$$

$$\Gamma_{lm}(\epsilon) = 16 JS_\infty \langle S_m^z \rangle G_{lm}(E), \quad \bar{S}_l = (S_\infty)^{-1} \langle S_l^z \rangle, \quad (4.6)$$

where J is the exchange constant for the interactions between nearest neighbors on opposite sublattices in the pure host and K is the anisotropy for the latter. One now has

$$\epsilon \Gamma_{lm}(\epsilon) = \frac{1}{\pi} \delta_{lm} + \alpha_l \bar{S}_l \Gamma_{lm}(\epsilon) + \frac{1}{8} \sum_{k(l)} j_{lk} [\bar{S}_l \Gamma_{km}(\epsilon) - \bar{S}_k \Gamma_{lm}(\epsilon)]. \quad (4.7)$$

For l on the up and down lattices, respectively, these equations may be arranged in the form

$$(\epsilon - 1 - \alpha) \Gamma_{gm}(\epsilon) - \frac{1}{8} \sum_{f(g)} \Gamma_{fm}(\epsilon) = (1/\pi) \delta_{gm} + (\alpha_g \bar{S}_g - \alpha) \Gamma_{gm}(\epsilon) + \frac{1}{8} \sum_{f(g)} [(j_{gf} \bar{S}_g - 1) \Gamma_{fm}(\epsilon) - (j_{gf} \bar{S}_f + 1) \Gamma_{gm}(\epsilon)] \\ \equiv (1/\pi) \delta_{gm} + P_{gm}, \\ (\epsilon + 1 + \alpha) \Gamma_{fm}(\epsilon) + \frac{1}{8} \sum_{g(f)} \Gamma_{gm}(\epsilon) = (1/\pi) \delta_{fm} + (\alpha_f \bar{S}_f + \alpha) \Gamma_{fm}(\epsilon) + \frac{1}{8} \sum_{g(f)} [(j_{fg} \bar{S}_f + 1) \Gamma_{gm}(\epsilon) - (j_{fg} \bar{S}_g - 1) \Gamma_{fm}(\epsilon)] \\ \equiv (1/\pi) \delta_{fm} + Q_{fm}.$$

We shall label the site occupied by the impurity as "0" and assume it to be on the up sublattice. The terms P_{gm} and Q_{fm} in Eq. (4.8) would vanish in the absence of the impurity; they now fail to do so for two reasons. Since the interactions between the impurity and the anisotropy of the impurity will not, in general, have the values typical of the host, j_{0f} and α_0 will differ from 1 and α , respectively. Hence P_{0m} and $Q_{f(0)m}$ will differ from zero. In addition, the presence of the impurity will, in principle, change every \bar{S}_g and \bar{S}_f from its normal value. Thus, every P_{gm} and Q_{fm} departs from zero to some extent. A complete solution of the impurity problem would entail solving the infinite set of equations for the Γ 's in terms of the \bar{S}_g and \bar{S}_f , which, in turn, would have to be calculated self-consistently from the Γ_{gg} and Γ_{ff} . Clearly, this is not feasible and one must eventually replace the original problem by a tractable model. In practice, this means we must assume that the \bar{S} 's are negligibly different from ± 1 beyond some definite distance from the impurity.

Formally, if one regards Γ as a matrix, Eqs.

(4.8) have the form

$$M\Gamma = (1/\pi)1 + C\Gamma, \quad (4.9)$$

where

$$M = \begin{vmatrix} \epsilon - 1 - \alpha & -\frac{1}{8}\Delta \\ \frac{1}{8}\Delta & \epsilon + 1 - \alpha \end{vmatrix} \quad (4.10)$$

and Δ is a (square) matrix with unit elements between nearest-neighbor sites on opposite sublattices. M is partitioned, in this case, by sublattices. C is the perturbation matrix whose elements are the P_{gm} 's and Q_{fm} 's. If the approximation mentioned above has been made of ignoring the differences $\bar{S}_g - 1$ and $\bar{S}_f + 1$, beyond some definite distance from the impurity, C is a finite matrix. Here "finite" means not of the order of the number of lattice sites.

Γ^0 , the solution for Γ in the pure crystal, is clearly given by

$$\Gamma^0 = (1/\pi)M^{-1}. \quad (4.11)$$

Thus, (4.9) may be rewritten as

$$\Gamma = \Gamma^0(1 + \pi C\Gamma) \quad (4.12)$$

and has the formal solution

$$\Gamma = (1 - \pi\Gamma^0 C)^{-1}\Gamma^0. \quad (4.13)$$

The matrix Γ^0 , the pure crystal Green's function, is given in the form

$$\Gamma^0 = \frac{1}{\pi} \begin{vmatrix} (\epsilon + 1 + \alpha)U_\epsilon & V_\epsilon \\ -V_\epsilon & (\epsilon - 1 - \alpha)U_\epsilon \end{vmatrix}, \quad (4.14)$$

where the partitioning is again by sublattices. Here we have

$$U_\epsilon(\vec{g} - \vec{g}') = \frac{1}{N} \lim_{\delta \rightarrow 0^+} \sum_{\vec{k}} \frac{e^{-i\vec{k} \cdot (\vec{g} - \vec{g}')}}{(\epsilon + i\delta)^2 - (1 + \alpha)^2 + \gamma(\vec{k})^2}, \quad (4.15)$$

$$V_\epsilon(\vec{g} - \vec{f}') = \frac{1}{N} \lim_{\delta \rightarrow 0^+} \sum_{\vec{k}} \frac{e^{-i\vec{k} \cdot (\vec{g} - \vec{f}')}}{(\epsilon + i\delta)^2 - (1 + \alpha)^2 + \gamma(\vec{k})^2}. \quad (4.16)$$

N is the number of sites on one sublattice, \vec{k} is a reciprocal-sublattice vector, and $\gamma(\vec{k}) = \frac{1}{8} \sum_{\delta_i} e^{i\vec{k} \cdot \delta_i}$, where the δ_i are the displacements to a nearest neighbor on the opposite sublattice. $\epsilon^2 = (1 + \alpha)^2 - \gamma(\vec{k})^2$ is the dispersion relation for spin waves in the body-centered antiferromagnet and in a finite system U and V would have poles at the spin-wave energies. As was remarked earlier, if we proceed to the limit of an infinite system before allowing δ to go to zero, U and V become complex within the spin-wave band, $(2\alpha + \alpha^2)^{1/2} < |\epsilon| < 1 + \alpha$. The functions U and V are obviously of basic importance in this problem and their evaluation forms a substantial part of the computational task.⁷

From Γ^0 one can obtain the pure-host magnetiza-

tion S_∞ . One has, in fact,

$$\Gamma_{gg}^0 = (1/\pi)(\epsilon + 1 + \alpha)U_\epsilon(0), \quad (4.17)$$

and from Eqs. (3.7)–(3.9) S_∞ is determined by the two relations

$$S_\infty = (S + \frac{1}{2}) \coth(S + \frac{1}{2})y - \frac{1}{2} \coth \frac{1}{2}y \quad (4.18)$$

and

$$\frac{1}{e^y - 1} = \frac{1}{\pi} \int_{-\infty}^{+\infty} \frac{d\epsilon}{e^{(16J\beta S_\infty)\epsilon} - 1} (\epsilon + 1 + \alpha) \text{Im } U_\epsilon(0), \quad (4.19)$$

where S is the magnitude of the host spin and $\beta = (kT)^{-1}$, where k is Boltzmann's constant. If we let $16J\beta S_\infty$ be denoted by w , it is clear that y and, subsequently, S_∞ can be found for a given w . Knowing w and S_∞ , one can find β or T . Thus S_∞ and T are found parametrically in terms of w . The RPA decoupling, combined with the Callen-Shtrikman prescription, gives a definite Néel temperature for the system. In fact, we have

$$\frac{kT_N}{J} = \frac{16\pi S(S+1)}{3(1+\alpha)} \left(\int_{-\infty}^{+\infty} \frac{[-\text{Im } U_\epsilon(0)]}{\epsilon} d\epsilon \right)^{-1}.$$

The behavior of S_∞ near T_N is of the form $(T_N - T)^{1/2}$ reflecting the molecular field character of (4.18).

Suppose the matrix C has been reduced to finite dimension by cutting off the disturbance of the \bar{S}_g 's and \bar{S}_f 's beyond some shell surrounding the impurity. We may write now

$$\left[\begin{pmatrix} 1 & 0 \\ 0 & 1 \end{pmatrix} - \pi \begin{pmatrix} \Gamma_a^0 & \Gamma_b^0 \\ \Gamma_c^0 & \Gamma_d^0 \end{pmatrix} \begin{pmatrix} C & 0 \\ 0 & 0 \end{pmatrix} \right] \begin{pmatrix} \Gamma_a & \Gamma_b \\ \Gamma_c & \Gamma_d \end{pmatrix} = \begin{pmatrix} \Gamma_a^0 & \Gamma_b^0 \\ \Gamma_c^0 & \Gamma_d^0 \end{pmatrix}, \quad (4.20)$$

where the partitioning now simply segregates the set of sites between which C is supposed to have matrix elements. From this, one may obtain Γ_a and Γ_d , which contain the diagonal elements of Γ , in the form

$$\Gamma_a = (1 - \pi\Gamma_a^0 C)^{-1}\Gamma_a^0 = \Gamma_a^0 + \pi\Gamma_a^0 C(1 - \pi\Gamma_a^0 C)^{-1}\Gamma_a^0 \quad (4.21)$$

and

$$\Gamma_d = \Gamma_d^0 + \pi\Gamma_d^0 C(1 - \pi\Gamma_d^0 C)^{-1}\Gamma_d^0. \quad (4.22)$$

If we indicate by "i" sites between which C has matrix elements and by "j" all others, we have

$$\Gamma_{ii} = \sum_{i'} (1 - \pi\Gamma_a^0 C)^{-1}_{ii'} \Gamma_{i',i}^0, \quad (4.23)$$

$$\Gamma_{jj} = \Gamma_{jj}^0 + \sum_{i, i', i''} \pi\Gamma_{ji}^0 C_{ii'} (1 - \pi\Gamma_a^0 C)^{-1}_{i''i} \Gamma_{i'',j}^0. \quad (4.24)$$

The evaluation of the required elements of the Γ matrix now involves only the inversion of the finite matrix $(1 - \pi\Gamma_a^0 C)$. One could, in principle, now calculate those S 's within the cluster which differ

from the host value, using some initial assumed values for these \bar{S} 's as a start. The procedure would be iterated until self-consistency is obtained. Making use of such self-consistent \bar{S} 's, one may then evaluate Γ_{ii} and Γ_{jj} for the remaining sites to obtain estimates of the corresponding \bar{S} 's in order to verify the original approximation.

B. Local Modes and Resonances

When an impurity is introduced into the host lattice the magnetizations of sites which transform into one another under operations of the point symmetry group of the impurity are identical. Since this is the case the matrices Γ^0 , Γ , and C , or any truncated version of the latter produced by the method mentioned above, also have a symmetry property. This is simply that

$$X_{ij} = X_{R(i)R(j)}, \quad (4.25)$$

where R is an operation of the impurity point group and X is any one of the matrices mentioned. One may take advantage of this symmetry property to facilitate the diagonalization into block form of the matrix $(1 - \pi\Gamma_a^0 C)$ before inverting it. Each diagonal block will correspond to one of the irreducible representations of the point group. From the form of Eq. (4.22) it is clear that the singularities of Γ_a , in a large but finite system, will be given by the zeros of the determinant of $(1 - \pi\Gamma_a^0 C)$. These will be the excitation energies of the system containing the impurity. The block diagonalization corresponds to an initial sorting of these modes by symmetry type. If we index the blocks by μ we have

$$\begin{aligned} \text{Im}\Gamma_a^{(\mu)} &= \text{Im}[(1 - \pi\Gamma_a^0 C)^{(\mu)}]^{-1} \Gamma_a^{0(\mu)} \\ &\equiv \text{Im}[(1/D^{(\mu)})N^{(\mu)}\Gamma_a^{0(\mu)}], \end{aligned} \quad (4.26)$$

where the determinant $D^{(\mu)}$ and the matrix elements of $N^{(\mu)}$ and $\Gamma_a^{0(\mu)}$ are, in the quasicontinuous case, all complex numbers. We may expect to find peaks in $\text{Im}\Gamma_a^{(\mu)}$ under certain circumstances. Equation (4.26) has the form

$$\frac{\text{Im}[N^{(\mu)}\Gamma_a^{0(\mu)}(\text{Re}D^{(\mu)} - i\text{Im}D^{(\mu)})]}{(\text{Re}D^{(\mu)})^2 + (\text{Im}D^{(\mu)})^2},$$

which will peak near $\text{Re}D^{(\mu)}(\epsilon_0) = 0$, provided that in a range of

$$|\epsilon - \epsilon_0| \sim \left| \text{Im}D^{(\mu)} \right. / \left. \frac{\partial}{\partial \epsilon} \text{Re}D^{(\mu)} \right|_{\epsilon_0}$$

everything is slowly varying with ϵ . $\text{Re}D^{(\mu)}(\epsilon) = 0$ is the usual criterion for a "resonance," but, in real cases, the actual position of the peak may be substantially shifted.

Returning for a moment to Eq. (4.9), note that the discrete ϵ_α 's are the eigenvalues of $\det(M(\epsilon_\alpha) - C) = 0$ and thus, we have

$$\text{Tr}\Gamma = \frac{1}{\pi} \sum_{\alpha} \frac{1}{\epsilon - \epsilon_{\alpha}}. \quad (4.27)$$

Clearly, $-\text{Tr}\text{Im}\Gamma = -\sum_i \text{Im}\Gamma_{ii} = \rho(\epsilon)$, where $\rho(\epsilon)$ is the density of states. It is not inappropriate to look upon $-\text{Im}\Gamma_{ii}$ as a local state density at site i . We also have

$$\Gamma_{ii}(\epsilon + i\delta) = \frac{1}{\pi} \sum_{\alpha} S_{i\alpha} \frac{1}{\epsilon + i\delta - \epsilon_{\alpha}} S_{\alpha i}^{-1},$$

where S is unitary and hence,

$$-\int_{-\infty}^{+\infty} \text{Im}\Gamma_{ii}(\epsilon) d\epsilon = 1. \quad (4.28)$$

This is equivalent to the sum rule cited earlier.

If sharp excitations exist outside the continuum they correspond to real zeros of $\det(1 - \pi\Gamma_a^0 C)$ for energies outside the spin-wave band, where, of course, the determinant is real. Since $\det|M(\epsilon) - C| = \prod_{\alpha} (\epsilon - \epsilon_{\alpha})$, we may derive the relation

$$\Gamma_{ij} = \frac{1}{\pi} \sum_{\alpha} \frac{\partial \epsilon_{\alpha}}{\partial M_{ji}} \frac{1}{\epsilon - \epsilon_{\alpha}}. \quad (4.29)$$

For an isolated ϵ_{α} the contribution to $\text{Im}\Gamma_{ij}$ is $-(\partial \epsilon_{\alpha} / \partial M_{ji}) \delta(\epsilon - \epsilon_{\alpha})$ or $-\pi \delta(\epsilon - \epsilon_{\alpha}) (\partial \Gamma_{ij}^{-1} / \partial \epsilon)^{-1}$. The contribution of an isolated level to $\text{Im}\Gamma$ can thus be found by studying how Γ goes through zero at $\epsilon = \epsilon_{\alpha}$.

V. NUMERICAL ANALYSIS

A. Green's Functions and Computational Procedures

The calculation of the functions U and V has been described in a separate publication where tables of numerical values are given.⁷ The neglect of anything but nearest-neighbor exchange has the effect of making U and V functions of the combination of variables $(1 + \alpha)^2 - \epsilon^2$. Since it is necessary to carry out, many times, integrations over the continuum, which runs from $|\epsilon| = (2\alpha + \alpha^2)^{1/2}$ to $|\epsilon| = 1 + \alpha$, it is desirable to change the integration variable to $x = [(1 + \alpha)^2 - \epsilon^2]^{1/2}$, which runs from 0 at the top of the band to 1 at the bottom in all cases. Subdividing the interval from 0 to 1 into subintervals and selecting various numbers of points in each as ordinates for Gaussian quadrature we obtained a set of points at which the Green's function was evaluated. The choice which was made was not perhaps the most judicious. It was based on consideration of the behavior of the pure-crystal Green's function which has a rather strong divergence at the band edge. This, in turn, stems from the fact that in the bcc structure the frequency of the spin waves goes to a constant value all over the zone boundary. Points were thus chosen to cluster tightly near the top of the band. However, the *impurity* Green's functions do not show any such peak since the impurity is indifferent to this particular frequency. Our calculation of integrals is therefore done some-

what inefficiently.

Outside the band, Green's functions are calculated as a function of $y = [\epsilon^2 - (1 + \alpha)^2]^{1/2}$. The number of points required here is difficult to predict. To calculate contributions to the various integrals from the localized modes it is necessary first to know where these lie, and second to know how fast Γ is changing at such energies. The modes lie at the zeros of $1/\Gamma_{ii}$, so one needs to locate these and to find the slope of $1/\Gamma_{ii}$ at the zeros. The procedure is to use equally spaced points in y , look for a change in sign of $1/\Gamma_{ii}$, then find the zero and the slope using a four-point interpolation formula.

All the calculations rely heavily on the existence of the sum rule (4.28). This serves as a check integral and has been evaluated simultaneously with every integral used in finding the S 's. A departure from unity in the check integral of more than 1% is indicative of trouble. Apart from program errors there is one basic source of difficulty which is revealed in this way. If a resonant mode lies deep in the spin-wave band, it may become extraordinarily sharp in energy; considerably less in half-width than the separation between the Gaussian ordinates. The integration routine may then fail suddenly by 15 or 20%. This has been allowed for by treating such peaks as δ functions; the error in the check integral measures the strength of this δ function. Other integrals which contain this peak multiplied by other factors are therefore corrected by the product of these factors and the strength of the peak. Fortunately, no cases have been encountered where there exist two such peaks, for which the above procedure would be useless.

In all the calculations the average value of the impurity moment is a quantity which is determined self-consistently by an iterative procedure. Assuming some initial value for this quantity the appropriate Green's functions are calculated within whatever approximation is being used. From these a new value of the moment is calculated and the cycle is repeated. In all cases three cycles of iteration are performed. The last two values, in general, agree to a few parts in a thousand. If the departure is greater than 1%, another cycle is made. Any failure to converge is indicative of program errors.

Two approximation schemes were used for solving the moment equations. The first of these will be described only briefly, since it was not extensively used. It is an extension of a method used earlier in the ferromagnetic problem.³ We include interactions between the impurity and its neighbors and between these neighbors and the three other shells to which they couple. The moments in these outer

shells are given the host value which has already been calculated. The neighbor moments are given by the following algorithm. The molecular field on a neighbor and on a host spin are compared and the difference field is supposed to produce a difference in moment at the two sites through a molecular field susceptibility. Knowing the neighbor moments and assuming a value for that of the impurity we calculate Γ_{00} and thus a new value for the impurity moment. This procedure is then iterated, correcting the neighbor moments in the same way at each stage. The matrix dimensionality is 5×5 since every site in each shell has the same moment. The method generates only an impurity moment and depends upon the unsatisfactory use of molecular field theory. For these reasons it was not pursued. It is of some interest to note that the values for the impurity moment obtained with it agreed very well with those found from the second method.

This second approach, upon which all the results reported here are based, is in some ways less accurate than the first but produces much more information. Here we assume that all spins except the impurity have the host thermal average value. The perturbation matrix is 9×9 since it connects the impurity to its eight neighbors. This matrix may be inverted explicitly making use of its symmetries. Thus the various Γ_{ii} 's may be found as a sum of terms each arising from a different symmetry. There is one term associated with two s symmetries, one associated with three degenerate p symmetries, one with three d symmetries, and one with an f symmetry. The Γ 's may be used to calculate the impurity moment and those of the first four shells. In the operation of the program Γ_{00} is first found, assuming a value of S_0 , the impurity moment, and is used to generate a corrected value. The cycle is repeated until S_0 converges. Then with the final value of S the other Γ_{ii} 's are found and hence the corresponding S_i 's. Clearly the usefulness of this method depends upon the moments in neighboring shells being only slightly altered from the host value. More precisely it requires that the change in the properties of the medium as a result of the actual changes in the neighboring shell spins be small.

We now write out explicitly the expressions given by this model for the various Γ_{ii} 's of interest. For a host spin we have noted earlier that Γ , which we shall call Γ_∞ , is given by

$$\pi\Gamma_\infty = (1 + \alpha + \epsilon)U(000) . \quad (5.1)$$

The impurity Green's function Γ_{00} may be written usefully in several different ways. In the form

$$\pi\Gamma_{00} = \frac{j_0 \bar{S} \pi \Gamma_\infty - (1 - j_0 \bar{S}_0)[1 + (\alpha - \epsilon)\pi\Gamma_\infty]}{j_0 - (\epsilon - \alpha_0 \bar{S}_0)(1 - j_0 \bar{S}_0)[1 + (\alpha - \epsilon)\pi\Gamma_\infty] - j_0[(\epsilon - \alpha) - (\epsilon - \alpha_0 \bar{S}_0)S_0]\pi\Gamma_\infty} , \quad (5.2)$$

it is clear that Γ_{00} reverts to Γ_{∞} when the impurity is identical to the host or $j_0 = \bar{S}_0 = 1$ and $\alpha_0 = \alpha$. Another form is

$$\pi\Gamma_{00} = \frac{1 - j_0\bar{S}_0Q}{\epsilon - j_0 - \alpha_0\bar{S}_0 - (\epsilon - \alpha_0\bar{S}_0)j_0\bar{S}_0Q} = \frac{1 - j_0\bar{S}_0Q}{\Delta}, \quad (5.3)$$

where

$$Q = \frac{1 + \alpha - \epsilon}{V(111)^{-1} + \alpha - \epsilon}. \quad (5.4)$$

This may be manipulated to read

$$\pi\Gamma_{00} = \frac{1}{\epsilon - \alpha_0\bar{S}_0 - j_0} + \frac{j_0^2\bar{S}_0(1 + \alpha - \epsilon)}{(\epsilon - \alpha_0\bar{S}_0 - j_0)^2} \frac{1}{V(111)^{-1} + \alpha - \epsilon - j_0\bar{S}_0(1 + \alpha - \epsilon)(\epsilon - \alpha_0\bar{S}_0)/(\epsilon - \alpha_0\bar{S}_0 - j_0)}. \quad (5.5)$$

Since $V(111)$ is the only complex term in this expression, it is simple to derive a form for $\text{Im}(\pi\Gamma_{00})$. The nominal location of the s modes, localized or resonant, is given by the vanishing of

$$\text{Re}[V(111)^{-1}] + \alpha - \epsilon - \frac{j_0\bar{S}_0(1 + \alpha - \epsilon)(\epsilon - \alpha_0\bar{S}_0)}{\epsilon - \alpha_0\bar{S}_0 - j_0}. \quad (5.6)$$

(It is clear that by symmetry only s modes couple to the impurity.) If the mode is localized (outside the continuum), then $\text{Im}[V(111)^{-1}]$ vanishes and the above condition is exact. As remarked earlier, the size of $\text{Im}[V(111)^{-1}]$ near an in-band resonance and the rate of change of the expression of (5.6) with ϵ near its zero may shift the observed maximum in $\text{Im}\Gamma_{00}$ quite considerably. A table of values of $V(111)^{-1}$ clearly enables one to examine any particular impurity problem for the behavior of the s modes before a detailed calculation is started. Figure 1 gives this information. The large number of parameters in the problem makes it impossible to reduce the mode analysis to simple form, but if α is held fixed, one can make a plot of $\text{Re}[V(111)^{-1}] + \alpha - \epsilon / (1 + \alpha - \epsilon)$ as a function of ϵ . Figure 2 shows such a plot for $\alpha = 0.0142$ (close to that for MnF_2). The positions of the s modes are now given by the intersection of this curve with $j_0\bar{S}_0[1 + j_0/(\epsilon - \alpha_0\bar{S}_0 - j_0)]$ which is just a rectangular hyperbola with a positive asymptote $j_0\bar{S}_0$ and a pole at $\epsilon = \alpha_0\bar{S}_0 + j_0$. It is rather easy now to see how the mode energies will vary with changes in various parameters by sketching the corresponding hyperbolae. It is worth repeating that the vanishing of the real part of the denominator of Γ may lead to a very broad and scarcely observable peak in $\text{Im}\Gamma$. In commenting on the results we shall refer only to in-band modes which give substantial peaks in $\text{Im}\Gamma$. In most cases which we have considered there is an in-band s mode with negative energy (easily deduced from Fig. 2), but this is invariably barely perceptible in the spectral weight function.

For the localized modes we can conveniently write

$$\frac{1}{\pi\Gamma_{00}} = \epsilon - \alpha_0\bar{S}_0 - \frac{j_0}{1 - j_0\bar{S}_0(1 + \alpha - \epsilon)/[V(111)^{-1} + \alpha - \epsilon]}, \quad (5.7)$$

and draw two useful conclusions from this form. If the mode lies well above the spin-wave band ($\epsilon \gg 1$) the corresponding $V(111)$ is small. $V(111)$, in fact, behaves like $1/(8\epsilon^2)$ for large ϵ . Thus one may write

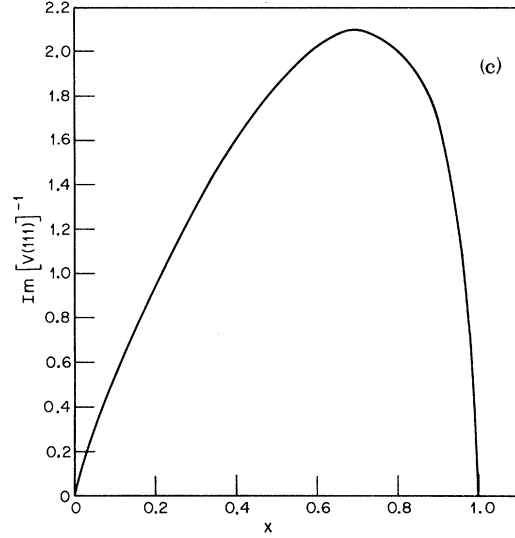
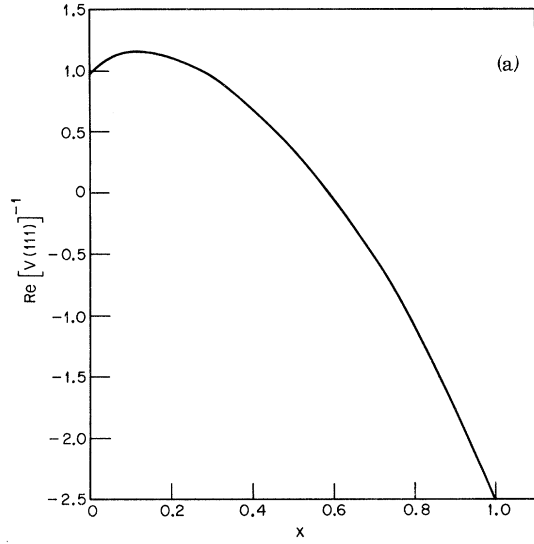
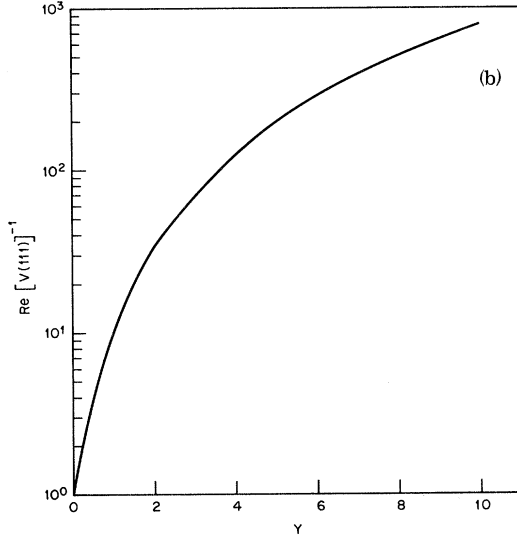
$$\epsilon \sim j_0 + \alpha_0\bar{S}_0 - j_0^2\bar{S}_0[V(111)]_{j_0 + \alpha_0\bar{S}_0} (j_0 + \alpha_0\bar{S}_0 - 1 - \alpha) \quad (5.8)$$

and

$$\frac{\partial}{\partial \epsilon} \left(\frac{1}{\pi\Gamma_{00}} \right) \sim 1 - j_0^2\bar{S}_0 \frac{\partial}{\partial \epsilon} [(1 + \alpha - \epsilon)V(111)]_{j_0 + \alpha_0\bar{S}_0}. \quad (5.9)$$

The first relation says that ϵ lies close to the molecular field energy ($j_0 + \alpha_0\bar{S}_0$) and the second relation says that the in-band contribution to $-\text{Im}\Gamma_{00}$ is close to unity. The sum rule for $-\text{Im}\Gamma_{00}$ now tells us either that $\text{Im}\Gamma_{00}$ is small for $\epsilon > 0$ and for $\epsilon < 0$, or that these two contributions are substantial but cancel. The former alternative is the one which occurs in practice. Clearly, the validity of these statements has to be checked in specific cases but the general trend is clear. It follows that in cases where a localized s mode exists well outside the band the thermal demagnetization of the impurity will proceed in two stages. At low temperatures the only excitations are into the low-lying continuum, but since the spectral weight is low, the magnetization will fall very slowly. If thermal excitation of the localized level becomes possible before the Néel temperature is reached, the demagnetization will be dominated rapidly by this process and will follow roughly the law $\delta\langle S \rangle \sim e^{-\epsilon_{\text{local}}/kT}$.

The thresholds for the appearance of localized s modes or conditions under which such modes just begin to emerge from the continuum may readily be deduced from the above expressions. Such relations have been derived by other authors⁸ and we do not

FIG. 1. Real and imaginary parts of $[V(111)]^{-1}$.

$$C_1 = (\epsilon - 1 - \alpha)[U(000) + U(100) - U(110) - U(111)] ,$$

$$C_2 = (\epsilon - 1 - \alpha)[U(000) - U(100) - U(110) + U(111)] ,$$

$$C_3 = (\epsilon - 1 - \alpha)[U(000) - 3U(100) + 3U(110) - U(111)] . \quad (5.11)$$

The first term represents the contribution of s -like terms and has the same denominator as occurred in Γ_{00} . The second, third, and fourth terms are the p -, d -, and f -like contributions. The vanishing of the real parts of their denominators give the nominal positions of the corresponding p , d , and f resonances or local modes. These are usually referred to as the shell modes. Conditions for the formation of local modes have been given by Tonegawa and Kanamori.⁸ In Fig. 3, the real part of $8/C_i$ is shown for $i=1, 2, 3$. The reducibility of Γ_{11} to the appropriate form for a down spin in the host when $j_0 = \bar{S}_0 = 1$ and $\alpha_0 = \alpha$ is readily demonstrated. It should be noted that $\epsilon < 0$ for all shell modes; no confusion should arise if we speak of them as "rising" in energy when $|\epsilon|$ increases.

The three outer shells considered are those for which a typical spin lies at $(1, 0, 0)$, $(1, 1, 0)$, and $(1, 1, 1)$, respectively. The corresponding Γ 's are labelled Γ_{22} , Γ_{33} , and Γ_{44} and the magnetizations are called S_2 , S_3 , S_4 . It is more convenient to write these Γ 's as Γ_∞ plus a correction term. We find

repeat them here.

We shall write Γ_{11} for the Γ of a spin in the nearest-neighbor shell. It is given by

$$\pi\Gamma_{11} = \frac{-(\epsilon - j_0 - \alpha_0 \bar{S}_0)Q}{\Delta} + \frac{3C_1}{8 - (1 - j_0 \bar{S}_0)C_1} + \frac{3C_2}{8 - (1 - j_0 \bar{S}_0)C_2} + \frac{C_3}{8 - (1 - j_0 \bar{S}_0)C_3} , \quad (5.10)$$

where the abbreviation Δ was introduced in Eq. (5.3) and

$$\pi\Gamma_{nn} = \pi\Gamma_\infty - (\epsilon + 1 + \alpha)^2 U(n)^2 \frac{1 + \alpha - \epsilon - (\epsilon - \alpha)Q}{\Delta} [j_0 \bar{S}_0 (\epsilon - 1 - \alpha)(\epsilon - \alpha_0 \bar{S}_0) - (\epsilon - j_0 - \alpha_0 \bar{S}_0)]$$

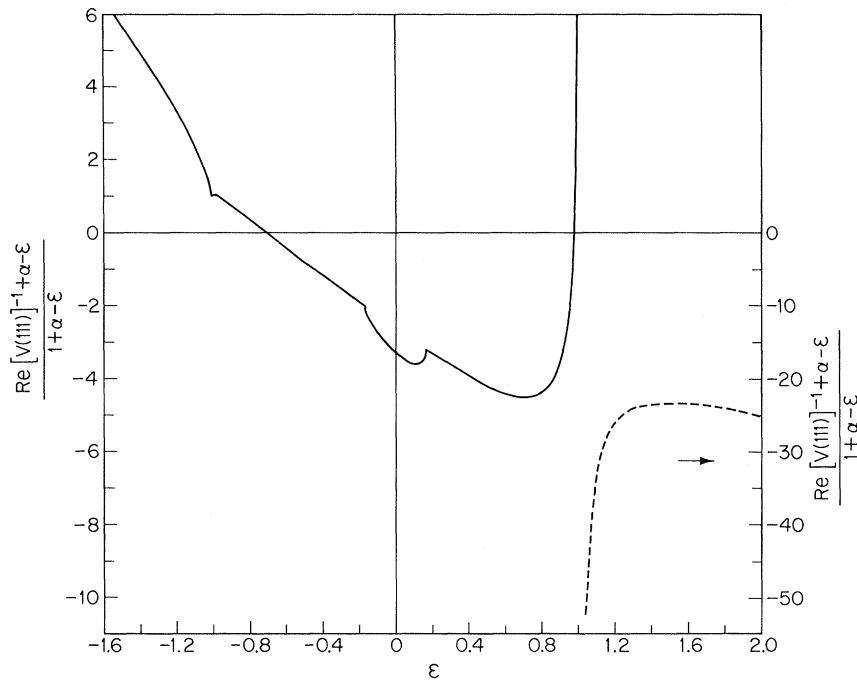


FIG. 2. $\text{Re}[V(111)]^{-1+\alpha-\epsilon} / (1+\alpha-\epsilon)$ vs ϵ for $\alpha=0.0142$. Band limits are $0.169 < |\epsilon| < 1.0142$.

$$-(1-j_0\bar{S}_0) \left(\frac{A_{n1}}{8-(1-j_0\bar{S}_0)C_1} + \frac{A_{n2}}{8-(1-j_0\bar{S}_0)C_2} + \frac{A_{n3}}{8-(1-j_0\bar{S}_0)C_3} \right), \quad (5.12)$$

where $U(1) = U(100)$, $U(2) = U(110)$, $U(3) = U(111)$, and the A 's are given by

$$\begin{aligned} A_{21} &= 0, \\ A_{22} &= 2[V(111) - V(113)]^2, \\ A_{23} &= 0, \\ A_{31} &= \frac{1}{2}[V(111) - 2V(113) + V(133)]^2, \\ A_{32} &= [V(111) - V(133)]^2, \end{aligned} \quad (5.13)$$

$$A_{33} = 0,$$

$$A_{41} = \frac{3}{8}[V(111) - V(113) - V(133) + V(333)]^2,$$

$$A_{42} = \frac{3}{8}[V(111) + V(113) - V(133) - V(333)]^2,$$

$$A_{43} = \frac{1}{8}[V(111) - 3V(113) + 3V(133) - V(333)]^2.$$

No new modes appear in these expressions since they are entirely dependent upon the inversion of the coupling matrix between the impurity and the nearest-neighbor shell in this approximate model.

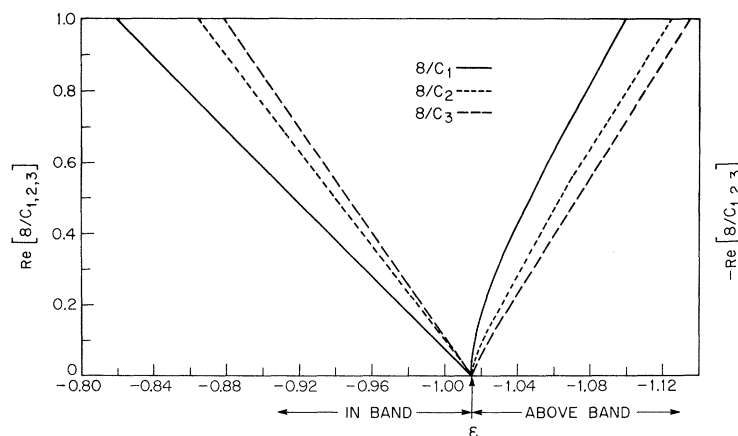


FIG. 3. Functions associated with the shell modes [see Eq. (5.11)]. $\text{Re}[8/C_{1,2,3}] \leq 0$ when $\epsilon \geq -1.0142$. Only $\text{Re}[8/C_{1,2,3}] < 1$ can yield a mode. "Above Band" implies $|\epsilon| > |\alpha|$.

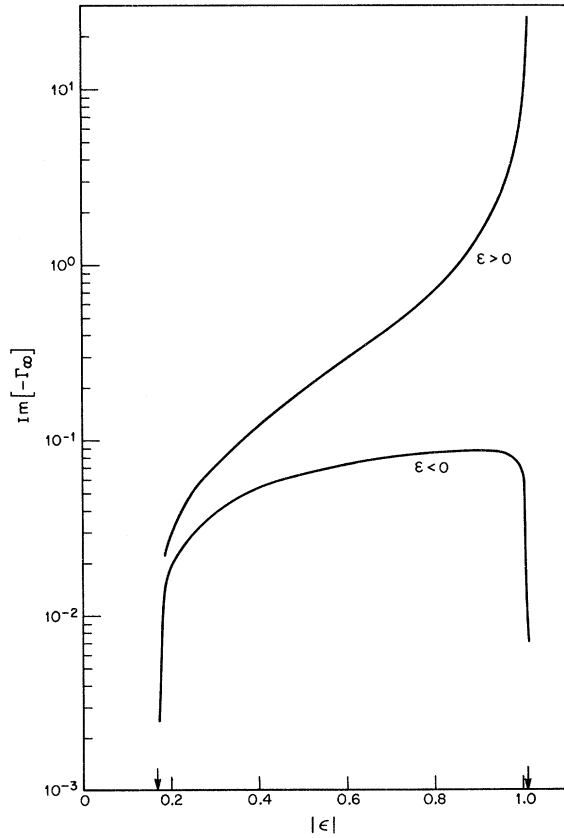


FIG. 4. $-\text{Im}\Gamma$ for the pure host. Band limits are indicated by arrows. $\alpha = 0.0142$.

Since the same localized modes (if there are any) occur repeatedly in the calculation of the various Γ 's, we calculate the zeros and derivatives with respect to ϵ of the denominators Δ and $8 - (1 - j_0 \bar{S}_0) \times C_{1,2,3}$ once and multiply the latter by appropriate constants for the different Γ 's.

VI. IMPURITY AND NEIGHBOR MAGNETIZATIONS

It has been pointed out earlier that since these calculations consider only exchange between nearest neighbors they are not primarily directed toward a comparison with experiment. A certain amount of information exists, in fact, concerning impurities in MnF_2 , and we shall discuss these results in the light of our analysis. Such a discussion is understood to be illustrative only since we are simulating the physical system with a one-exchange model. Clearly, since we have a five-parameter (S , the host spin; Σ , the impurity spin; j_0 ; α ; and α_0) family of possible problems, it is not feasible to make an exhaustive survey of these. What we have done is to consider a number of informative cases. We shall describe the results of these calculations below and discuss them in a rather discursive way, pointing out anything which seems significant.

Before starting this discussion we show in Fig. 4 $\text{Im}\Gamma$ for the uniform case (or $\text{Im}\Gamma_\infty$) with $\alpha = 0.0142$. Note that it has a singularity at the upper edge ($\epsilon = 1 + \alpha$) of the positive energy band, which arises because the spin-wave frequency goes to the same value over the whole zone boundary. This singularity disappears for the impurity since the symmetry which the zone boundary reflects has now disappeared.

It is useful to discuss first the introduction of an impurity whose spin is the same as that of the host and which also has the same anisotropy. The exchange coupling between the impurity and the host is allowed to vary. Specifically, we let the host and impurity have spin $\frac{5}{2}$ and let the anisotropy parameter α be 0.0142. The host, therefore, is like MnF_2 . We have considered the cases $j_0 = 1.5, 1.25, 0.75, 0.50, 0.18$, and 0.06 and we discuss them in that order. Figure 5 shows the host magnetization and Fig. 6 shows the impurity magnetization \bar{S}_0 as a function of temperature for all cases. The temperature is normalized to the Néel temperature. Figure 7 shows the function $\text{Im}\Gamma_{00}$ as a function of ϵ for all values of j_0 at a very low temperature ($t = 0.0537$).

When $j_0 > 1$ a localized s mode exists above the spin-wave band. The condition for this to happen, in general, is simply that the molecular field energy $j_0 + \alpha_0 \bar{S}_0$ exceeds the energy $1 + \alpha$ at the zone boundary. In the present cases of $j_0 = 1.5$ and $j_0 = 1.25$, the mode lies at $\epsilon \sim 1.4$ and $\epsilon \sim 1.2$. The known condition for the shell modes to lie above the continuum is $j_0 \bar{S}_0 > 1$ and this is also fulfilled in

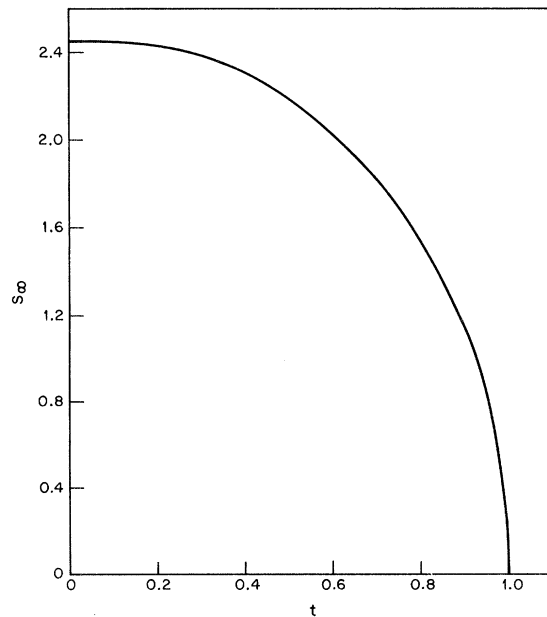


FIG. 5. Magnetization of pure host as a function of the reduced temperature ($t = T/T_N$) for $\alpha = 0.0142$ and $S = \frac{5}{2}$.

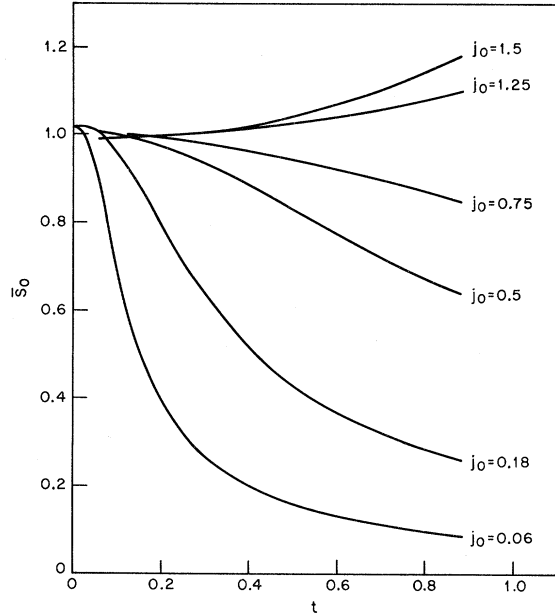


FIG. 6. Ratio of impurity-to-host magnetization \bar{S}_0 as a function of reduced temperature ($t = T/T_N$) for various values of the impurity-host exchange j_0 . $S = \Sigma = \frac{5}{2}$, $\alpha = \alpha_0 = 0.0142$.

these two cases. We note at this point the rather obvious fact that, since the positions of the localized modes and resonant peaks depend upon \bar{S}_0 which is itself a function of temperature, these positions themselves are temperature dependent. In particular, it is quite possible for a localized mode to move into the continuum (or out of it) as the temperature changes. Since such changes depend upon the *ratio* of impurity-to-host magnetization they are not, in general, very rapid. It should be recalled that the absolute energy of a mode depends linearly upon the bandwidth (or, in the RPA, to the host magnetization) and this gives the dominant temperature dependence.

It will be seen that for $j_0 = 1.5$ and 1.25 the zero-point deviation of the impurity magnetization is greater than that of the host, but that the decline with increasing temperature is less. It is slower for $j_0 = 1.5$ than for $j_0 = 1.25$. To understand the latter fact it is instructive to compare $-\int \text{Im}\Gamma_\infty d\epsilon$ in various regions. For the host at low temperatures this is -0.0538 from all negative ϵ and 1.0538 from all positive ϵ . For $j_0 = 1.5$ we get -0.0713 from negative ϵ , $+0.0790$ from positive ϵ , and 0.993 from the localized mode above the band; for $j_0 = 1.25$ the corresponding numbers are -0.0633 , $+0.1213$, and $+0.942$. Thus the localized mode plays a completely dominant role in controlling the thermal behavior. The Boltzmann factor for this mode is e^{-1} at $T/T_N = 0.83$ for the

$j_0 = 1.5$ case; for substantially lower temperatures the magnetization is supported by the reduced possibility of continuum excitation. The motion of the localized level with temperature is quite small (of the order of 2% over the temperature range covered). The shell modes move up by about 10% as \bar{S}_0 grows with temperature, reflecting the dominant role of the factor $1 - j_0 \bar{S}_0$ in their resonance condition. In Table I are shown the magnetizations of the impurity and its four neighbor shells in terms of the host magnetization at different temperatures. It will be noted that the magnetizations of shells 2, 3, and 4 are altered by less than 1% over the whole range. This turns out to be generally the case and we shall only comment on those cases where it fails to be true. That this result should be obtained lends considerable support to the type of approximation we have used.

The fact that the zero-point deviation of the impurity is greater than that of the host in this case may be understood, and the magnitude of the effect

TABLE I. Magnetizations of impurity and four neighbor shells relative to that of the host as a function of reduced temperature. $S = \Sigma = \frac{5}{2}$, $\alpha = \alpha_0 = 0.0142$, $t = T/T_N$.

J_0	t	\bar{S}_0	$-\bar{S}_1$	\bar{S}_2	\bar{S}_3	\bar{S}_4
1.50	0.0537	0.9928	0.9998	1.0008	1.0000	1.0000
	0.2636	1.0014	1.0021	1.0010	1.0005	1.0001
	0.4830	1.0406	1.0117	1.0016	1.0010	1.0003
	0.6801	1.0980	1.0287	1.0027	1.0017	1.0008
	0.8826	1.1853	1.0600	1.0044	1.0030	1.0017
1.25	0.0537	0.9961	0.9993	1.0004	0.9994	1.0000
	0.2636	1.0022	1.0111	1.0005	1.0002	1.0000
	0.4830	1.0265	1.0062	1.0007	1.0004	1.0002
	0.6801	1.0598	1.0150	1.0011	1.0007	1.0004
	0.8826	1.1067	1.0312	1.0017	1.0012	1.0008
0.75	0.0537	1.0047	1.0000	0.9998	0.9999	0.9999
	0.2636	0.9891	0.9986	0.9997	0.9997	0.9998
	0.4830	0.9483	0.9930	0.9992	0.9993	0.9996
	0.6801	0.9026	0.9838	0.9982	0.9986	0.9992
	0.8826	0.8519	0.9688	0.9966	0.9973	0.9985
0.50	0.0537	1.0103	0.9993	0.9996	0.9997	0.9998
	0.2636	0.9510	1.0015	0.9994	0.9995	0.9997
	0.4830	0.8379	0.9778	0.9985	0.9987	0.9992
	0.6801	0.7349	0.9726	0.9969	0.9975	0.9985
	0.8826	0.6426	0.9514	0.9943	0.9954	0.9972
0.18	0.0537	1.0087	1.0133	0.9993	0.9995	0.9997
	0.2636	0.6863	0.9830	0.9986	0.9989	0.9991
	0.4830	0.4484	0.9552	0.9981	0.9983	0.9990
	0.6801	0.3309	0.9479	0.9957	0.9965	0.9981
	0.8826	0.2602	0.9280	0.9925	0.9937	0.9964
0.06	0.0269	0.9991	0.9996	0.9991	0.9993	0.9993
	0.0537	0.8916	0.9995	0.9991	0.9993	0.9997
	0.2636	0.2967	1.0109	0.9986	0.9989	0.9994
	0.4830	0.1629	0.9952	0.9970	0.9976	0.9986
	0.6801	0.1155	0.9741	0.9946	0.9957	0.9974
0.8826	0.0889	0.9439	0.9909	0.9928	0.9958	

predicted roughly, by a simple second-order perturbation calculation. If we treat the Néel state as the ground state and the transverse exchange as a perturbation, then in the absence of anisotropy, we find for the ratio of impurity deviation (Δ_{imp}) to host deviation (Δ_{host})

$$\frac{\Delta_{\text{imp}}}{\Delta_{\text{host}}} = \left(\frac{\Sigma}{S} \right) \frac{(16S-1)^2}{[(8+7/j_0)S+\Sigma-1]^2}, \quad (6.1)$$

where S is the host spin and Σ is the spin of the impurity. For $\Sigma = S = \frac{5}{2}$ one has

$$\frac{\Delta_{\text{imp}}}{\Delta_{\text{host}}} = \left(\frac{78}{43+35/j_0} \right)^2. \quad (6.2)$$

When $\Sigma = S$ the sign of $\Delta_{\text{imp}} - \Delta_{\text{host}}$ reverses as j_0 goes through unity. The deviation to this order is proportional to the ratio of the square of the matrix element for flipping the spin in question and one of its neighbors to the square of the excitation energy for this process. The former is proportional to j_0 but the latter is the sum of two positive terms, only one of which is proportional to j_0 . As j_0 increases the deviation also increases. Or, succinctly, to flip a weakly coupled spin one must also turn over some normally coupled spins.

For the cases $j_0 = 0.75$ and 0.50 , there is a qualitative change in the spectrum since no local modes now exist. There is a resonant peak in $\text{Im}\Gamma_{00}$ at $\epsilon \sim 0.75$ for the first case and at $\epsilon \sim 0.48$ for the second. The resonance can be seen (Fig. 7) to get higher and sharper as j_0 decreases. As was predicted by Eq. (6.2) the impurity magnetization starts above that of the host. It now falls more rapidly with temperature than the latter, as the resonant peak becomes lower in energy. When $j_0 = 0.3$ the resonance has fallen to $\epsilon \sim 0.184$; it now lies just above the bottom of the continuum which occurs at $\epsilon = (2\alpha + \alpha^2)^{1/2} = 0.169$. The resonance is now exceedingly sharp and would be experimentally no different from a localized level. The magnetization of the impurity, of course, now falls even more rapidly. Finally, for $j_0 = 0.06$, the s mode has become localized again, but is now in the spin-wave gap. At this point the fall off in magnetization is so rapid that the decrease in zero-point deviation is already masked at the lowest temperature which we use.

Throughout this sequence the position of the s -mode level continues to be insensitive to temperature. The shell modes remain close together, quite high up in the band ($-\epsilon \sim 0.8 - 0.95$); they therefore cause no drastic effects on the magnetization of the neighbors. Table I shows the magnetization of impurity and first-shell spins in terms of the host for all the cases considered. Effects on the first-shell spins are seen to be less than 10% in all cases; the change in these spins is seen to follow

\bar{S}_0 . Or, an impurity which is "stiffer" than the host holds up the nearest-neighbor magnetization. The results quoted for near neighbors are probably somewhat unreliable for small j_0 . This is caused by the fact that the p , d , and f shell resonances have now become quite sharp and lie close to one another. This makes accurate integration difficult without special provision. This problem will arise again when the effect of a vacancy is considered.

Consider now a case in which the impurity-host exchange equals the host-host value, but let the impurity spin differ from that of the host. Specifically, we put $\Sigma = 1$ and $S = \frac{5}{2}$. Again $\alpha = \alpha_0 = 0.0142$. The impurity magnetization and that of the host are shown in Fig. 8 as a function of t and that of the nearest neighbors in Table II. $\text{Im}\Gamma_{00}$ for $t = 0.0537$ is shown in Fig. 9. The zero-point deviation is predicted quite well by Eq. (6.1); the magnetization then falls off more rapidly than that of the host and is comparable with that for $j_0 \sim 0.55$ in the first series. The drop in nearest-neighbor magnetizations is, however, more nearly that of $j_0 \sim 0.18$ in the earlier set. It may be remarked that the ratio of the s -mode contribution to $\text{Im}\Gamma_{11}$ and to $\text{Im}\Gamma_{00}$ is given generally by $(\epsilon - \alpha_0 \bar{S}_0 - j_0)^2 / j_0^2 \bar{S}_0$. In the present case there are no localized modes in the normal sense; there is a sharp s resonance just below the top of the band and the three shell modes are also high up. The s -mode resonance lies very close to the molecular field energy $j_0 + \alpha_0 \bar{S}_0$. We note that this value for the resonance energy and the decoupling of the s mode from its surroundings imply one another. In the present case the impurity resonance is occurring near the band edge so that it is coupled to zone-boundary spin waves which can accommodate a highly local excitation.

Suppose now that in the last case j_0 is changed to 3, so that one has a small spin impurity tightly coupled. The localized s mode now lies far above the band at $\epsilon \sim 2.89$. The approximate formula (5.8) gives 2.88 for this case. There is actually a fairly substantial absolute correction to the molecular-field value of 3 here. It may be noted that as j_0 tends to a very large value the s -mode position is given from Eq. (5.8) by

$$\epsilon = j_0(1 - \bar{S}_0/8) + \frac{\alpha_0 \bar{S}_0}{1 - \bar{S}_0/8}. \quad (6.3)$$

This indicates that a very tightly coupled spin is "dressed" by its neighbors. If one uses the formula given in the last paragraph it is easily shown that the s mode contributes to $\text{Im}\Gamma_{11}$ a fraction ($\frac{1}{84} \bar{S}_0$) of its contribution to $\text{Im}\Gamma_{00}$ as $j_0 \rightarrow \infty$, reflecting its extreme localization.

Because of the height of the local s mode the magnetization falls slowly (Fig. 8). The local s

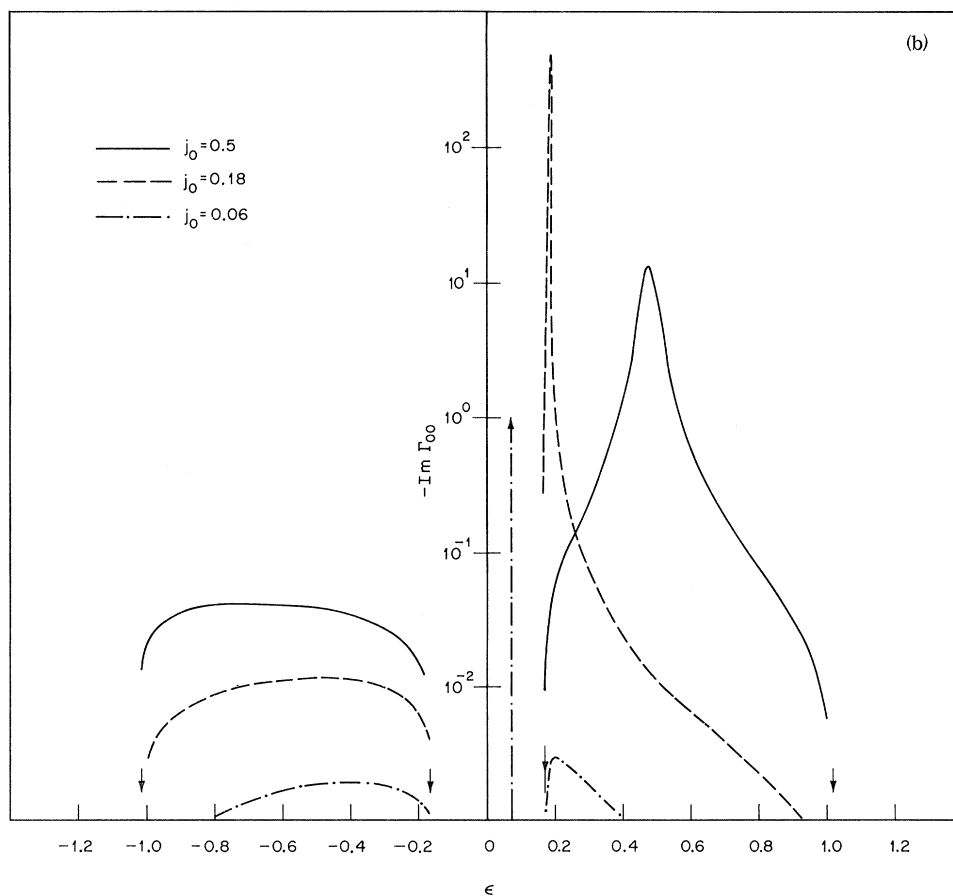
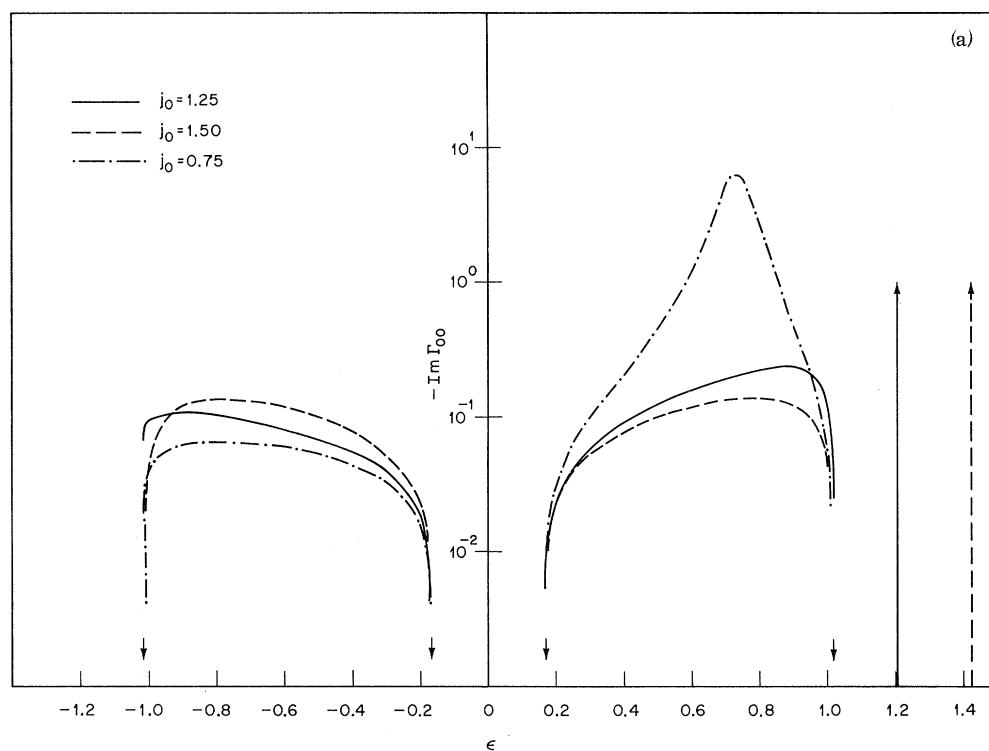


FIG. 7. $-\text{Im} \Gamma_{00}$ as a function of ϵ for various values of the impurity-host exchange j_0 . $S = \Sigma = \frac{5}{2}$, $\alpha = \alpha_0 = 0.0142$, $t = 0.0537$. δ functions corresponding to localized modes are shown as vertical lines arbitrarily terminated at $-\text{Im} \Gamma_{00} = 1$.

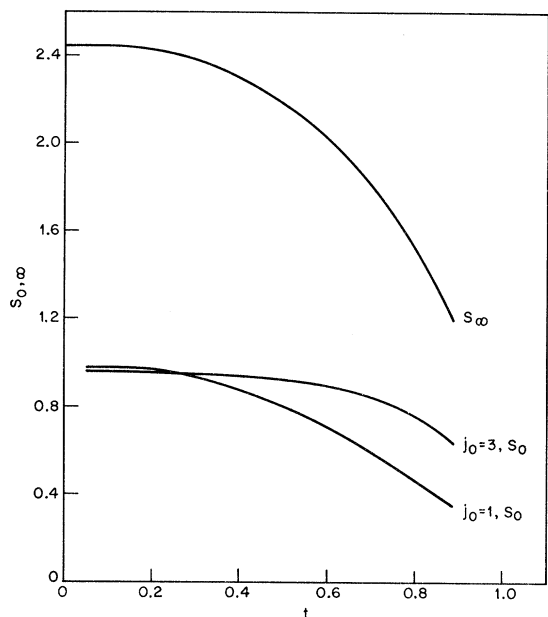


FIG. 8. Host magnetization S_∞ and impurity magnetization S_0 as a function of the reduced temperature ($t = T/T_N$) for two values of impurity-host exchange j_0 . $S = \frac{5}{2}$, $\Sigma = 1$, $\alpha = \alpha_0 = 0.0142$.

mode moves very little with temperature but the three shell modes which are above the band climb as \bar{S}_0 increases. The magnetizations of the nearest

neighbors (see Table II) remain unusually close to the host value in this case. Figure 9 shows $\text{Im}\Gamma_{00}$ vs ϵ .

Some cases will now be examined for which the host spin is $\frac{1}{2}$. We take $\alpha = \alpha_0 = 0.02$ and first consider two examples with Σ also equal to $\frac{1}{2}$ and $j_0 = 0.5$ and 1.5 , respectively. The cases are perhaps not judiciously chosen for comparison with the earlier ones in which $\Sigma = S = \frac{5}{2}$ because the anisotropy term has been altered. This change raises the bottom of the band from $\epsilon = 0.169$ to 0.20 , which has some effect on the low-temperature response. Otherwise we are dealing with two situations with the same saturation value of \bar{S}_0 ; departures in the results arise from the relative sensitivity of small and large spins to roughly the same spin-wave excitations.

The results for these two cases are shown in Table III and should be compared with those for $\Sigma = S = \frac{5}{2}$ in Table I. It is clear that the over-all behavior is much the same for both. The present example shows that the impurity magnetization falls more rapidly now for a weak exchange and more slowly than before with strong exchange. The position of the s , p , d , and f resonances turn out to be very closely equal for both spin values, hence the implied differences in $\text{Im}\Gamma_{00}$ for the two cases must arise from the numerator or amplitude factor alone. The zero-point deviations follow the rule given earlier. They are 0.0268 for $j_0 = 0.5$ and 0.0600 for $j_0 = 1.5$; the host value is 0.0472 and

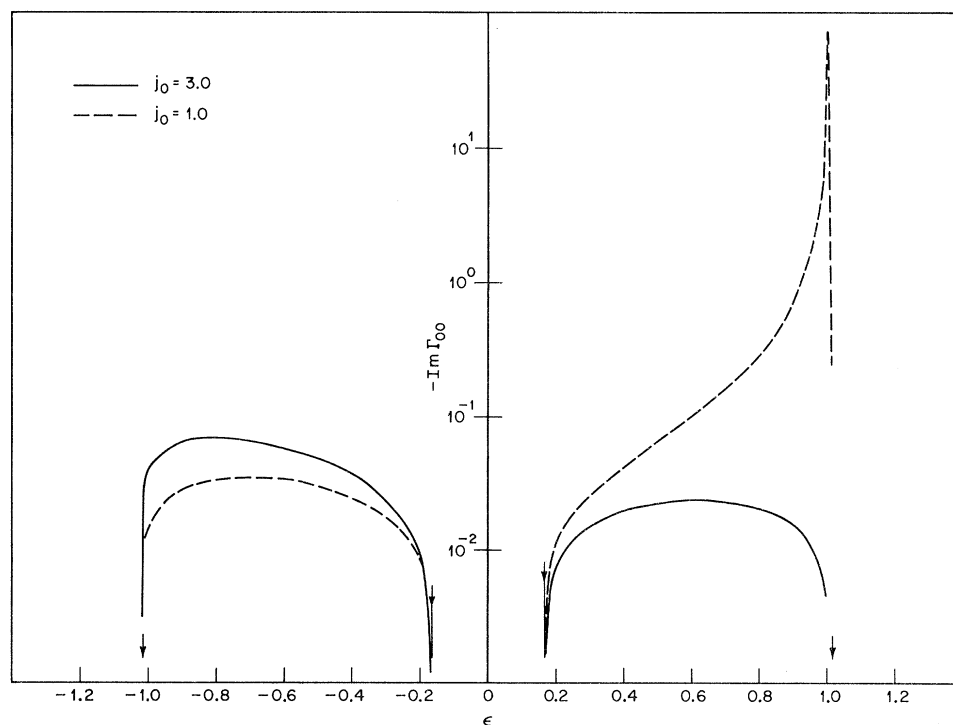


FIG. 9. $-\text{Im}\Gamma_{00}$ as a function of ϵ for two values of the impurity-host exchange j_0 . $S = \frac{5}{2}$, $\Sigma = 1$, $\alpha = \alpha_0 = 0.0142$, $t = 0.0537$. Localized mode for $j_0 = 1.5$ lies at $\epsilon = 2.90$ and is not shown.

TABLE II. Magnetizations of impurity and four neighbor shells relative to that of the host as a function of reduced temperature. $\Sigma=1$, $S=\frac{5}{2}$, $\alpha=\alpha_0=0.0142$, $t=T/T_N$.

J_0	t	\bar{S}_0	$-\bar{S}_1$	\bar{S}_2	\bar{S}_3	\bar{S}_4
3.0	0.0537	0.3925	1.0006	1.0000	1.0000	1.0000
	0.2636	0.3965	1.0012	1.0002	1.0000	1.0000
	0.4830	0.4207	1.0057	1.0006	1.0003	1.0001
	0.6801	0.4620	1.0173	1.0013	0.9984	1.0004
	0.8826	0.5277	1.0459	1.0029	1.0020	1.0011
1.0	0.0537	0.3997	0.9942	0.9994	0.9996	0.9998
	0.2636	0.3953	0.9910	0.9992	0.9994	0.9996
	0.4830	0.3660	0.9885	0.9982	0.9986	0.9992
	0.6801	0.3283	0.9760	0.9966	0.9973	0.9983
	0.8826	0.2908	0.9262	0.9940	0.9952	0.9969

the simple perturbation-calculation algorithm given above yields 0.021 and 0.068. Figure 10 shows $\text{Im}\Gamma_{00}$ vs ϵ .

As a final model system a spin of 1 is put into a spin- $\frac{1}{2}$ host. Again $\alpha=\alpha_0=0.02$. We consider again $j_0=0.5$ and $j_0=1.5$. Table III shows the results and Fig. 11 shows $\text{Im}\Gamma_{00}$ vs ϵ . For $j_0=0.5$ there is nothing unusual; the impurity magnetization again falls more rapidly than the host. The s resonance lies at $\epsilon\sim 0.470$ which compares with a value of $\epsilon\sim 0.483$ at which it occurred in the $j_0=0.5$, $\Sigma=\frac{1}{2}$ case above. This again shows the insensitivity of the s level to the value of \bar{S}_0 under certain conditions. In this case the p , d , and f levels are

TABLE III. Magnetizations of impurity and four neighbor shells relative to that of the host as a function of reduced temperature. $\Sigma=S=\frac{1}{2}$, $\alpha=\alpha_0=0.02$, $t=T/T_N$.

J_0	t	\bar{S}_0	$-\bar{S}_1$	\bar{S}_2	\bar{S}_3	\bar{S}_4
1.5	0.1139	0.9717	0.9991	1.0034	1.0015	0.9999
	0.5305	1.0047	1.0082	1.0042	1.0021	1.0003
	0.7975	1.1124	1.0395	1.0054	1.0032	1.0011
	0.9140	1.1847	1.0669	1.0058	1.0038	1.0017
	0.9774	1.2343	1.0770	1.0059	1.0040	1.0022
0.5	0.1139	1.0452	0.9881	0.9985	0.9988	0.9993
	0.5305	0.8447	0.9647	0.9972	0.9977	0.9984
	0.7975	0.6854	0.9815	0.9952	0.9961	0.9975
	0.9140	0.6301	0.9436	0.9940	0.9951	0.9968
	0.9774	0.6033	0.9192	0.9930	0.9944	0.9964

$\Sigma=1$, $S=\frac{1}{2}$, $\alpha=\alpha_0=0.02$

1.5	0.1139	1.9320	0.9951	1.0107	1.0051	1.0011
	0.5305	1.9931	1.0233	1.0119	1.0065	1.0023
	0.7975	2.2204	1.1201	1.0146	1.0094	1.0048
	0.9140	2.3873	1.1970	1.0160	1.0112	1.0065
	0.9774	2.5041	1.2601	1.0166	1.0122	1.0076
0.5	0.1139	2.0960	0.9996	1.0017	1.0007	1.0000
	0.5305	1.8430	1.0004	1.0003	1.0000	1.0000
	0.7975	1.6207	0.9893	0.9991	0.9991	0.9995
	0.9140	1.5370	0.9809	0.9982	0.9984	0.9992
	0.9774	1.4994	0.9751	0.9974	0.9978	0.9989

right at the band edge, which is to be expected since $j_0\bar{S}_0\sim 1$. The zero-point deviation is 0.051 which is not in particularly good agreement with

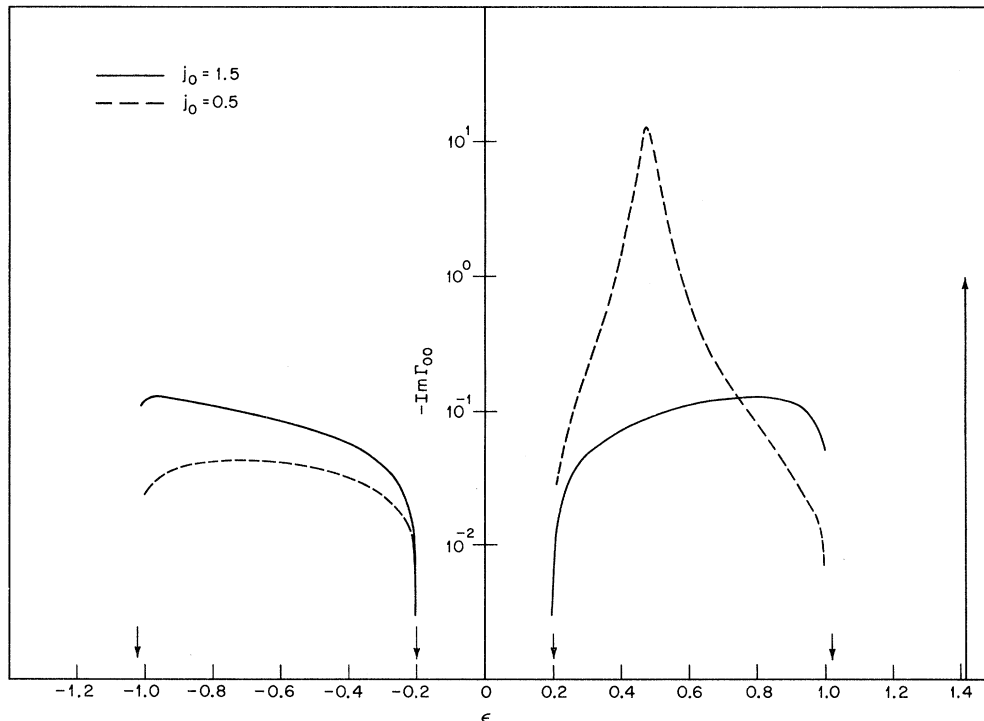


FIG. 10. $-\text{Im}\Gamma_{00}$ as a function of ϵ for two values of the impurity-host exchange j_0 . $S=\Sigma=\frac{1}{2}$, $\alpha=\alpha_0=0.02$, $t=0.1139$. δ function corresponding to a localized mode for $j_0=1.5$ is shown as a vertical line arbitrarily terminated at $-\text{Im}\Gamma_{00}=1$.

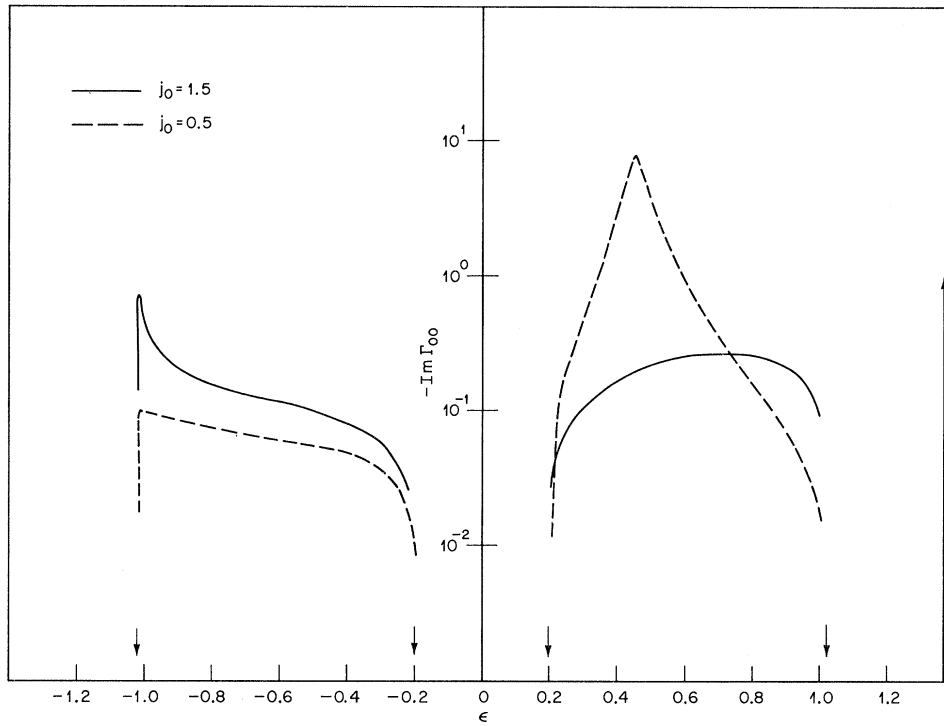


FIG. 11. $-\text{Im}\Gamma_{00}$ as a function of ϵ for two values of the impurity-host exchange j_0 . $S = \frac{1}{2}$, $\Sigma = 1$, $\alpha = \alpha_0 = 0.02$. δ function corresponding to a localized mode for $j_0 = 1.5$ is shown as a vertical line arbitrarily terminated at $-\text{Im}\Gamma_{00} = 1$.

perturbation theory which gives 0.038. The nearest-neighbor magnetization suffers little change at any temperature. For $j_0 = 1.5$ most of the features already noted appear in an emphasized way. The

zero-point deviation is 0.125 and the algorithm gives 0.115. The impurity is particularly stiff in this instance; the nearest neighbors are shifted by as much as 25% at high temperatures; the outer

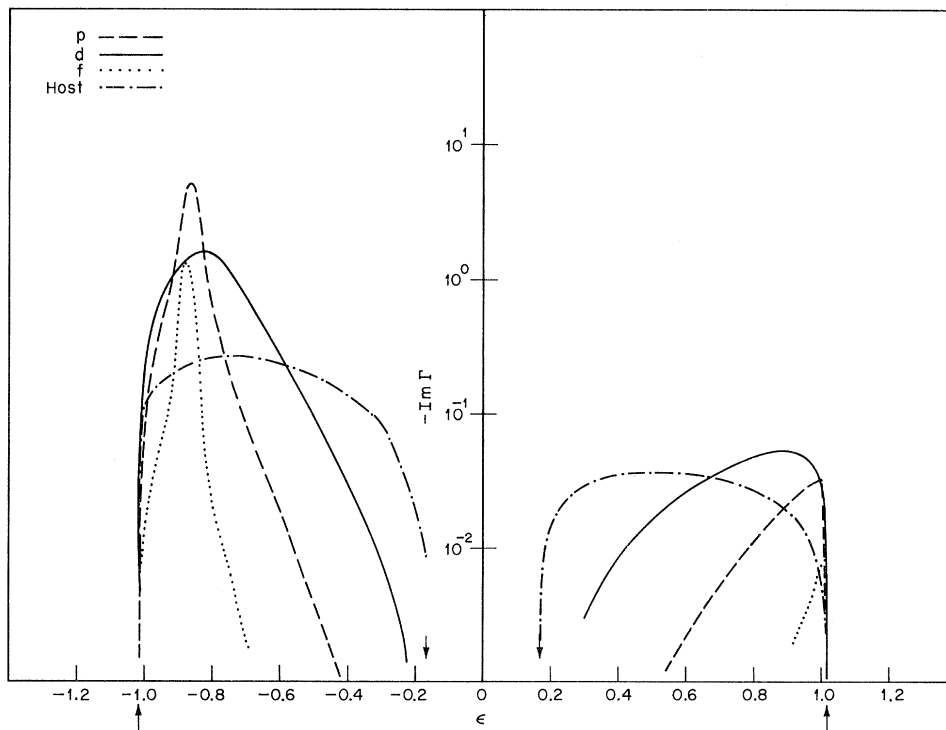


FIG. 12. Contributions to $-\text{Im}\Gamma_{11}$ for a nonmagnetic impurity. $S = \frac{3}{2}$, $\alpha = 0.0142$. Four curves labeled host p , d , and f correspond to the four terms of Eq. (5.10).

shells have a maximum shift of 1.5%—this being the only model to give anything over 1%. The spectrum here shows a new feature. In addition to the expected localized s mode above the band there is a second localized s mode at negative energies lying just above $\epsilon = -1 - \alpha$. The three shell modes lie within the band but their position is unusually temperature dependent. This is presumably because with a stiff impurity \bar{S}_0 changes considerably with temperature and hence $1 - j_0 \bar{S}_0$ also changes, pulling the shell modes with it. The condition that an s mode shall emerge below $\epsilon = -1 - \alpha$ is that⁸

$$(j_0 \bar{S}_0 - 1)(1 + \alpha + \alpha_0 \bar{S}_0) > j_0 \quad (6.4)$$

or

$$\bar{S}_0 > 1/j_0 + 1/(1 + \alpha + \alpha_0 \bar{S}_0). \quad (6.5)$$

Thus, for modest values of α and α_0 this occurs when we have an impurity with a nominal spin substantially greater than that of the host which is tightly ($j_0 > 1$) coupled. Such an s mode has its intensity mainly on the nearest-neighbor atoms. We have already seen that the relative contributions of the s mode to the near neighbors and to the impurity is $(\epsilon - \alpha_0 \bar{S}_0 - j_0)^2 / j_0^2 \bar{S}_0$; at $\epsilon = -1 - \alpha$ we can transform this with the aid of the threshold condition into $\bar{S}_0(1 + \alpha + \alpha_0 \bar{S}_0)^2$ which is indeed > 1 . To some extent this is true of all negative energy s

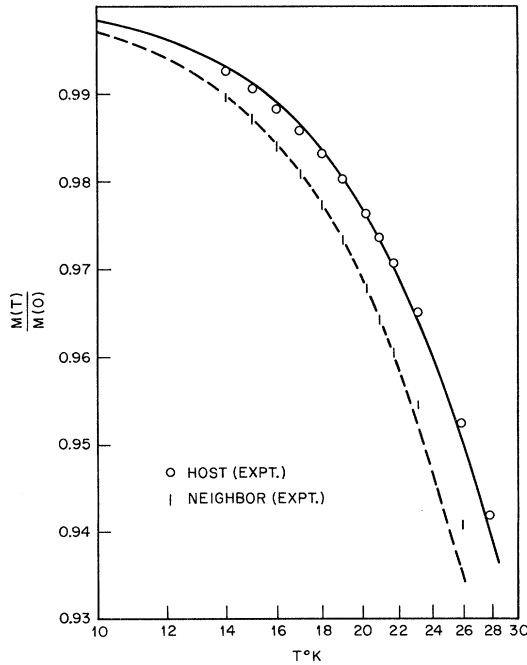


FIG. 13. Magnetization of Mn ions in MnF_2 which are far away from or nearest neighbors of Zn impurities. Experimental points are those of Butler *et al.* (Ref. 4). Solid and dashed curves are computed with the Mn-Mn exchange taken to be 1.320 cm^{-1} .

modes and, in fact, accounts for their weak contribution to the impurity magnetizations.

We now consider some cases which are related to experiment. The first case is that in which the impurity is nonmagnetic. Suppose $\bar{S}_0 = 0$, then Δ in Eq. (5.3) becomes $\epsilon - j_0$ and $\pi\Gamma_{00} = (\epsilon - j_0)^{-1}$. This simply implies that a very small \bar{S}_0 would precess in the molecular field j_0 without any modification resulting from a reaction of the rest of the spin system. Γ_{11} now becomes

$$\pi\Gamma_{11} = \frac{\epsilon - 1 - \alpha}{\epsilon - V(111)^{-1} - \alpha} + \frac{3C_1}{8 - C_1} + \frac{3C_2}{8 - C_2} + \frac{C_3}{8 - C_3}. \quad (6.6)$$

The positions of the s mode for the case where $\alpha = 0.0142$, which is relevant to MnF_2 , are $\epsilon = -0.704$ and $\epsilon = 0.971$, as found from $\epsilon - \alpha = \text{Re}[V(111)^{-1}]$. The former shows up very weakly because $\text{Im}[V(111)^{-1}]$ is large and $\text{Re}[V(111)^{-1}]$ varies slowly with energy near the critical value of ϵ . The latter is somewhat sharper but very weak because $\epsilon - 1 - \alpha$ is small. The main structure of Γ_{11} arises from the shell modes which are found to lie at $-\epsilon = 0.878, 0.865, \text{ and } 0.820$. The first (f) resonance is very sharp and it has to be estimated in strength by looking at the deficiency in the sum rule (see Fig. 12). The various shell mode contributions to $\text{Im}\Gamma_{11}$ are shown in Fig. 12. In Fig. 13, calculated values of $-S_1$, the first neighbor magnetization and S_∞ , that of the host are shown. We also show the values found for S_∞ in MnF_2 by Jaccarino^{8a} and for the magnetization of the nearest neighbor to a Zn impurity in MnF_2 by Butler *et al.*⁴ The value of J has been chosen to optimize the fit. The agreement is quite satisfactory. The single value of J so obtained is 1.320 cm^{-1} ; the best experimental values for J_1 and J_2 , the interactions between nearest neighbors (on the same sublattice along the c axis) and between next-nearest neighbors are -0.226 cm^{-1} and 1.225 cm^{-1} , respectively.⁹ The effective J for long wavelengths would then be essentially $1.225 + \frac{2}{8}(0.226)$ or 1.281 cm^{-1} . With the value of $\alpha = 0.0142$ which was used in our calculation the antiferromagnetic resonance frequency using $J = 1.320 \text{ cm}^{-1}$ is about 2.4% (higher than the measured value).¹⁰ The predicted Néel temperature is 69°K as compared to the experimental value of 67.34°K . Thus, the one-exchange-parameter theory gives a fairly adequate description of the system.

The deviations from the host value of the neighbors of the vacancy beyond the first shell are small. Typical values are from 0.1 to 0.2% in the second shell and 0.05 to 0.1% in the fourth shell.

Butler *et al.* have also measured the magnetiza-

tion of Ni impurities and their neighbors in MnF_2 . Attempts to fit this data making use of the known position of the localized level of Ni in MnF_2 , which lies far above the band¹¹ and of the crystal field parameters which have also been found, were not at all successful. It has been shown by Butler *et al.*⁴ that the observed magnetizations of neighbor spins strongly suggest that there is a large nearest-neighbor exchange between Ni and Mn. If this is the case then the present analysis is certainly not applicable.

There is some information available on Fe impurities in MnF_2 . Weber¹² has found a sharp local level at 94.8 cm^{-1} at 1.2°K . This lies substantially above the spin-wave band. Wertheim, Guggenheim, and Buchanan¹³ have measured the hyperfine splitting of the Mössbauer line of Fe in MnF_2 as a function of temperature up to $0.7T_N$. If it is assumed that the hyperfine constant is temperature independent (which may not be valid for an ion with large hyperfine orbital contributions), then the data measure the Fe magnetization.

A fit was made to this data essentially by trial and error. An estimate was made of the anisotropy field from data on Fe in a diamagnetic host¹⁴ and of the Fe-Mn exchange by comparison with the known Mn-Mn and Fe-Fe exchanges. These estimates served as starting values which were adjusted to improve the fit to the magnetization. The position of the local level was not used in this fitting but was afterwards predicted using our estimated value for the host J . The agreement between these calculations and experiment is shown in Fig. 14. It does not represent the very best that could be achieved but is satisfactory. The parameters used were $\alpha_0 = 0.4$ and $j_0 = 1.5$. With the value of J for the host which was estimated earlier this implies a $J_{\text{Mn-Fe}}$ of 1.971 cm^{-1} . This is rather close to the best molecular field estimate of Wertheim *et al.* of 1.87 cm^{-1} . This is not surprising. The position of the local mode at the lowest temperatures is $\epsilon = 1.425$ or 91.7 cm^{-1} . The value found by Weber¹² was 94.8 cm^{-1} . Since this local mode contains most of the spectral density, as soon as it becomes appreciably populated thermally it dominates the behavior of the system. At very low temperatures where only spin waves may be excited, the spectral density is very low and the fall-off of the magnetization is correspondingly slow. It is possible to estimate that at $\frac{1}{2}T_N$ the spin waves and the local mode are contributing about equally to the deficit in the magnetization.

Because the magnetization of the impurity falls off a good deal more slowly than that of the host, S_0 changes considerably with temperature and this shifts the resonances, both localized and in-band. It appears from this calculation that a second s mode which is rising steadily in the band as T decreases

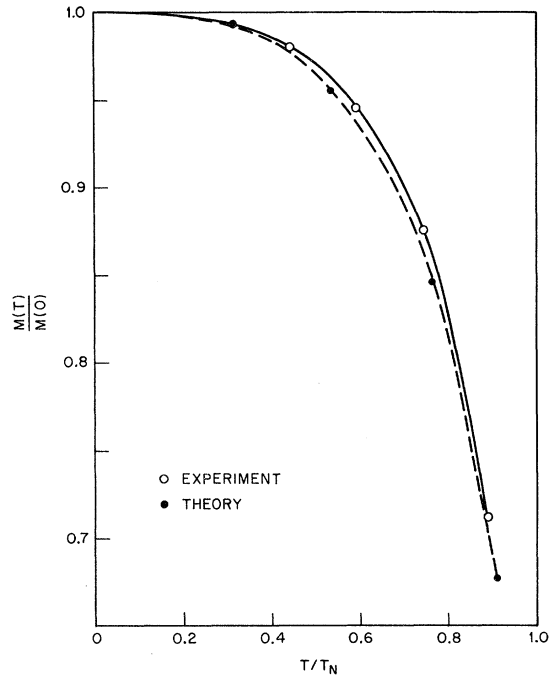


FIG. 14. Magnetization of Fe impurities in MnF_2 . Experimental points are Mössbauer hyperfine splittings from Wertheim *et al.* (Ref. 13).

may emerge from the latter just below the Néel temperature.

VII. CONCLUDING REMARKS

Probably the most valuable conclusion which can be drawn from these calculations is that the effect of impurities upon the magnetization of their neighbors is essentially significant only for nearest neighbors. The greatest shortcoming is undoubtedly the use of the RPA. This can be seen clearly from the results of the Chalk River group on a localized mode on Co in MnF_2 .¹⁵ Cobalt is a more complicated ion than those we have treated here, but this is probably not important. It was found that the position of the local level which lies well above the host spin-wave band (at 119 cm^{-1} for 4.6°K) falls only by 15% at $T/T_N = 0.8$, while the host band has narrowed by 40%. Since in the present analysis the position of such isolated modes remains essentially fixed in terms of the bandwidth, the RPA is clearly giving the wrong result.

The reason for this is rather clear. The work of Dyson¹⁶ and its physical interpretation by Keffer and Loudon¹⁷ showed that the renormalization of spin-wave frequencies proceeds more nearly with the average angle between neighbor spins than with the angle made by a spin with the direction of overall magnetization. It is reasonable to suppose that an impurity tightly coupled to its neighbors will have its local-mode frequency determined largely

by the angle which it makes with them. At low temperatures the effect of long-wavelength magnons will be to cause motions in which the impurity and

its neighbors move substantially as a unit preserving their mutual orientation. An improved theory would take this effect into account.^{18,19}

*Supported in part by the National Science Foundation.

†Supported in part by the U. S. Office of Naval Research and the National Science Foundation.

¹S. W. Lovesey, *J. Phys. C* **1**, 102 (1968); T. Tonegawa, *Progr. Theoret. Phys. (Kyoto)* **40**, 1195 (1968); E. Shiles and D. Hone, *J. Phys. Soc. Japan* **28**, 51 (1970).

²T. Wolfram and J. Callaway, *Phys. Rev.* **130**, 2207 (1963); T. Wolfram and W. Hall, *ibid.* **143**, 284 (1966).

³D. Hone, H. B. Callen, and L. R. Walker, *Phys. Rev.* **144**, 283 (1966).

⁴M. Butler, V. Jaccarino, N. Kaplan, and H. J. Guggenheim, *Phys. Rev.* **B1**, 3058 (1970); see also E. Shiles and D. Hone, Ref. 1.

⁵H. B. Callen, *Phys. Rev.* **130**, 890 (1963).

⁶H. B. Callen and S. Shtrikman, *Solid State Commun.* **3**, 5 (1965).

⁷L. R. Walker, B. B. Cetlin, and D. Hone, *J. Phys. Chem. Solids* **30**, 923 (1969).

⁸T. Tonegawa and J. Kanamori, *Phys. Letters* **21**, 130 (1966).

^{8a}V. Jaccarino (unpublished).

⁹O. Nikotin, P. A. Lindgard, and O. W. Dietrich, *J. Phys. C* **2**, 1168 (1969).

¹⁰F. M. Johnson and A. M. Nethercot, *Phys. Rev.* **104**, 847 (1956); **114**, 705 (1959).

¹¹L. F. Johnson, R. E. Dietz, and H. J. Guggenheim, *Phys. Rev. Letters* **17**, 13 (1966).

¹²R. Weber, *Phys. Rev. Letters* **21**, 1260 (1968).

¹³G. K. Wertheim, H. J. Guggenheim, and D. N. E. Buchanan, *J. Appl. Phys.* **40**, 1319 (1969).

¹⁴M. E. Lines, *Phys. Rev.* **156**, 543 (1967).

¹⁵T. M. Holden, W. J. L. Buyers, and R. W. H. Stevenson, *J. Appl. Phys.* **40**, 991 (1969).

¹⁶F. J. Dyson, *Phys. Rev.* **102**, 1217 (1955); **102**, 1230 (1955).

¹⁷F. Keffer and R. Loudon, *J. Appl. Phys.* **32**, 25 (1961).

¹⁸D. Hone, D. J. Scalapino, and R. Silbergliitt, *J. Appl. Phys.* **41**, 948 (1970).

¹⁹S. Watarai and T. Kawasaki (unpublished).

Electrical Resistivity and the Depression of the Néel Temperature in Cr-Mo and Cr-Fe

M. A. Mitchell and J. F. Goff

Naval Ordnance Laboratory, White Oak, Silver Spring, Maryland 20910

(Received 30 August 1971)

Existing data are used to show that Mo and Fe impurities cause the Néel temperature T_N of Cr to decrease at almost exactly the same rate up to 10 at.%. Elements with a higher valence than Cr generally increase T_N . It is suggested that two Fe electrons are localized and produce a localized magnetic moment, for which experimental evidence already exists. The effective valence of Fe would then be similar to that of Mo. In order to investigate the similarities and differences of Cr-Fe and Cr-Mo, electrical-resistivity measurements have been made on two Cr alloys with 9.35-at.% Mo and 9.35-at.% Fe, respectively, from 2 to 300°K. For Cr-Mo, $T_N=197^\circ\text{K}$, and for Cr-Fe, $T_N=181^\circ\text{K}$. At 0 and 200°K the resistivity of Cr-Fe is 12.6 and 3.2 times higher, respectively, than that of Cr-Mo. We suggest that localized magnetic moments at Fe sites combined with atomic disorder produce a large, nearly temperature-independent spin-disorder scattering in Cr-Fe. A simple model of electrical conduction is employed to explain the temperature dependence of the electrical resistivity. Below T_N an energy gap with a BCS temperature dependence opens up over a part of the Fermi surface, and conduction takes place in two bands. As a result of the gap, electrons in the magnetic band are thermally frozen out with decreasing temperature, which leads to the rise in resistivity just below T_N . The 0°K gap is estimated to be 0.14 eV for Cr-Mo and 0.072 eV for Cr-Fe. Pure Cr and Cr-Mo have nearly the same balance of conduction between the magnetic and nonmagnetic bands. In Cr-Fe the balance is shifted toward conduction in the magnetic band.

I. INTRODUCTION

The purpose of this paper is twofold. First we would like to point out that Mo and Fe impurities lower the Néel temperature T_N of chromium at almost exactly the same rate up to concentrations of the order of 10 at.%. This likeness does not

seem to have been noted before, although Suzuki has commented that there is an order-of-magnitude similarity.¹ Iron is anomalous since most other elements of higher valence than Cr cause T_N to increase.

Second, we report an analysis of the electrical resistivity of two Cr alloys containing 9.35 at.%